Title
Creating microenvironments with Claudins: The proper way to build gut and liver

Author
Cheung, Isla D.

Publication Date
2011

Peer reviewed|Thesis/dissertation

Creating microenvironments with claudins:

The proper way to build gut and liver

By

Isla D. Cheung

DISSERTATION

Submitted in partial satisfaction of the requirements for the degree of

DOCTOR OF PHILOSOPHY

in

Developmental Biology

in the

GRADUATE DIVISION

of the

UNIVERSITY OF CALIFORNIA, SAN FRANCISCO

[redacted]

Acknowledgements

I would like to first thank Didier Stainier, for being such a great thesis advisor. The first year of graduate school was difficult and he helped me pushed through it with his unwavering support. He continued to support all my scientific endeavors and provided all the necessary resources when I joined his lab. I cannot thank him enough for his scientific mentorship and guidance, and his care and understanding for my personal difficulties. In addition, I would like to thank Takashi Mikawa and Keith Mostov, members of my thesis committee, for providing valuable feedbacks on my projects and nurturing my scientific growth. I greatly appreciate our discussions about the science and my scientific career.

Next, I would like to thank members of the Stainier lab for their valuable discussions and insights, and more importantly, their friendship. Without their guidance and 'distractions', graduate school would have been so much tougher. I would like to especially thank Silvia Curado, Duc Dong, Tatiana Hochgreb, Won-Suk Chung, Chunyue Yin, and Stephanie Woo. A special thanks to Pia Aanstad and Michel Bagnat for taking me under their wings when I rotated and first joined the lab. I also deeply appreciate Ana Ayala and Milly Alva for helping me take care of my fish, without which this thesis is not possible! In addition, I would like to say 'thank you' to Kathleen Yamamoto, Sue Adams, Danny Dam, and Claire Manneh for providing all the 'behind-the-scene' support to make my graduate career so much smoother.

I am also very grateful for the friendship I have made through my graduate career. They were there for me for the good and bad times and have made such impact in my

life. Graduate school and my life definitely would not have been the same without them. A special shout-out for my fellow musketeers Karen Moreira and Rowena Suriben, Han Li, Linda Setiawan, and King Lee.

Lastly, I would like to say a big 'THANK YOU!!' and give a big hug to my family for their constant, unwavering confidence and support. I greatly appreciate all the big AND little things that you guys have done during the last few years. I don't think I could have finished my studies without it! Thank you for putting up with my emotional roller coasters and never leaving my side. Thank you Mommy. Thank you Daddy. Thank you Elman. I love you guys!

I would like to dedicate this dissertation to my immediate and extended family for all their care and support. Now, whenever you guys ask me when am I graduating, I can finally reply 'I have graduated!!' In memory of Ah Ma and Uncle Harry. I miss you guys.

Chapter 2

All portions of this chapter except introduction was originally published online July 15, 2007 and appeared in print August 9, 2007.

Bagnat, M., Cheung, I.D., Mostov, K.E., Stainier, D.Y. Genetic control of single lumen formation in the zxebrafish gut. Nat Cell Biol. 2007 Aug;9(8):954-60).

The article is available online at:

http://www.nature.com/ncb/journal/v9/n8/full/ncb1621.html

The research was directed and supervised by Didier Stainier and Keith Mostov. Isla Cheung participated in the microarray experiment, the microarray data analysis, analysis of wildtype zebrafish gut development in collaboration with Michel Bagnat. Isla Cheung conducted the expression analysis of *cldn15* and other genes of interest that arose from the microarray experiment. Michel Bagnat preformed the morpholino knockdown experiments, paracellular transport experiments, and the drug treatments affecting the electrochemical gradient.

Figure 3.4 b,c

Processing and staining of samples for electron microscopy were performed by Sandra Huling, M.S. at the Pathology & Imaging Core of the Liver Center at the University of California, San Francisco.

Creating microenvironments with claudins:

The proper way to build gut and liver

Isla D. Cheung

Abstract

While identifying genes necessary for organogenesis is important, having the appropriate cellular environment for cells to undergo morphogenesis is as important. Understanding the cell biology of zebrafish gut and liver development is the main interest of my thesis work. Claudins are junction proteins that are involved in the maintenance of polarity, the regulation of paracellular transport, and providing barrier functions. As such, they play a role in the establishment and maintenance of appropriate cellular environment by regulating the localization of different proteins or substances to their appropriate places. I have identified two claudins in my thesis work that are necessary for organ development.

During gut development, endodermal cells must rearrange themselves from an initial disorganized state to an organized radial pattern. I found that regulation of the dynamic localization of the adhesion proteins Cadherins may be important for mediating this process. After cells have arranged into a radial pattern, lumen that has formed at the apical region of these cells must coalesce to form a single lumen. We showed that the homeobox gene *tcf2* transcriptionally controls the expression of claudin15 and Na^+/K^+ ATPase to regulate single lumen formation. Together, claudin15 and Na^+/K^+ ATPase create the appropriate electrochemical microenvironment to drive fluid accumulation. In turn, the fluid accumulation drives lumen coalescence. Subsequently, the single lumen

must expand to form a functional gut tube. We provide evidence that apical membrane biogenesis is important for lumen expansion in gut development.

Another claudin, claudin15-likeb(cldn15lb), was found to have a dynamic expression pattern in the liver during development. Its initial expression in hepatocytes and biliary epithelial cells (BECs) becomes restricted to only the BECs at later stages of development. During biliary duct morphogenesis, BECs remodel to form a mature, functional network. Mutants of cldn15lb fail to remodel and form a disorganized biliary ductal network. Interestingly, these mutants do not have a severe polarity defect and can form tight junctions. The expression data and mutant phenotype suggest that cldn15lb may play a role in directing the remodeling process during biliary duct morphogenesis.

Table of Contents

List of Figures

List of Tables

Chapter 1:

Introduction

The epithelium is a tissue that functions as a barrier between an organism and the outside environment. It also compartmentalizes organs to efficiently maintain homeostasis. Epithelial cells of the digestive system are mostly columnar-shaped with distinct apico-basolateral polarity. A polarized cell contains an apical and a basolateral domain separated by junction complexes. One particular junction complex, the tight junction, is especially important for the function of the epithelium because they form intercellular seals that restrict paracellular transport. The claudin family of proteins is the main component of these tight junctions because they provide the structural and functional properties of the junction complex.

Epithelial morphogenesis is the driving force in formation of the body plan and the subsequent organ development. Complex processes such as cell rearrangement, proliferation and apoptosis, differentiation, polarization, and cell migration are utilized to form a functional epithelium. Some morphogenetic events require only one of these processes but most require multiple processes that occur in parallel or sequentially. In this dissertation, I studied the epithelial morphogenetic processes involved in zebrafish gut and biliary duct morphogenesis.

Claudins – Structure and Function

Tight junctions circumscribing the apex of polarized epithelial cells provide the barrier function of the epithelium. They form continuous intercellular seals that restrict

and regulate paracellular transport of large and small molecules. Tight junctions also serve as a fence to prevent diffusion of proteins and lipids between apical and basolateral membrane domains to maintain epithelial polarity. Claudins are core components of these tight junctions as they form and regulate the paracellular pore between epithelial cells. They are tetraspanning membrane proteins that were identified as calcium-independent adhesion molecules that mediate cell-cell contacts.[1] They can interact in cis or in trans and can interact with itself in a homomeric manner or with a different claudin in a heteromeric manner. The trans-interactions between claudins on neighboring cells are mediated by the extracellular loops. The amino acid composition of the first extracellular loop confers ionic properties and its interaction with neighboring claudins that form the paracellular pore determines the permeability selectivity of the pore. The intracellular c-terminal region of the protein contains a PDZ-binding domain that interacts with PDZ-containing scaffold proteins. These interactions stabilize the tight junctions.

Currently, 24 claudins have been identified in the mammals, 56 in pufferfish *Takifugu*, and at least 15 in zebrafish.[2] Distinct claudin expression profile in each tissue provides specialized functions important for that tissue. For example, in mouse, claudin-11 in sertoli cells functions in the blood-testis barrier. However, when co-expressed with claudin-19 in the myelin sheaths of oligodendrocytes and Schwann cells, it functions as an electrical sealing of myelin to assist saltatory conduction along axons.[3] Many studies have focused on understanding how interactions between different claudins can create a spectrum of barrier permeabilities. Furthermore, how claudins are assembled into tight junctions and their interactions with other tight junction

and scaffolding proteins are well characterized. An emerging field in claudin biology hypothesizes that there is crosstalk between claudin-containing tight junctions and the nucleus to regulate epithelial differentiation and proliferation.[4] However, most of these studies are done *in vitro* and the role of claudins *in vivo* is well understood.

Recent knockout mouse and zebrafish models have started to provide insight into the role of claudins in development.[3] Claudin-16 is expressed in the kidneys and mutation in this claudin causes defects in Mg^{2+} reabsorption.[5] In patients, it causes familial hypomagnesaemia with hypercalciuria and nephrocalcinosis.[5, 6] In the cochlear, Claudin-11 and -14 are expressed in an epithelium that form two distinct compartments.[7] The fluids in these compartments maintain different electric potentials which are important for hearing. Not surprisingly, knockout mice of Claudin-11 or -14 are deaf.[1, 8, 9] The intestine expresses several different claudins including Claudin-15.[10] Claudin-15 knockout mice survive to adulthood but have an abnormally longer intestine.[11] The mechanism resulting in this phenotype remains unknown. These studies suggest that claudins have two main roles *in vivo* - they regulate paracellular transport and provide barrier properties for compartmentalization. Both roles are indispensable for organ development and function.

Zebrafish gut morphogenesis

During zebrafish development, the endodermal epithelial sheet converges at the midline and extends to give rise to a rod of cells. To form a functional gut tube, a lumen is formed between cells of the cylindrical rod. Studies with caspase-3 indicate that apoptosis is not involved in this process. In a cross section view of this rod, the intestinal

tube is initially a collection of endodermal cells that are not polarized. Actin foci at points of cell-cell contact are observed. The cells then undergo rearrangement and organize into a radial pattern. During this rearrangement, actin foci appear to cluster together to a single focal point in the middle of the rod where it marks the site of future lumen formation.[12]

In the *aPKCλ* (also known as prkci) mutant *heart and soul*, actin foci fail to cluster together and the mutant gut tube exhibit a multiple lumen phenotype.[12] The phenotype suggests that polarization of the gut epithelium is intimately linked to cell rearrangement. Furthermore, the timing of the polarization during gut morphogenesis indicates its importance.[13] Polarization initiates with deposition of the basal protein laminin and subsequent localization of cadherin to the lateral membrane coincides with appearance of apical markers and actin foci clustering.[13]

Zebrafish biliary duct morphogenesis

The biliary ductal system is responsible for transporting bile from the liver to the digestive tract. Heritable biliary diseases such as Alagille syndrome, congenital hepatic fibrosis, and polycystic liver disease have defects in the formation of the biliary ductal system in the liver. In these diseases, bile flow is impaired causing bile to accumulate in the liver and ultimately causing liver damage. Thus, it is important to understand the mechanism through which the biliary ductal system is formed. While many studies have identified the signaling molecules and transcription factors involved in biliary epithelial cell (BEC) differentiation, less is known about the cellular behaviors that arrange them into a three-dimensional structure important for function.

The development of the mammalian biliary ductal system utilizes an integrated program of cell differentiation and polarization. BEC precursors initially align with the portal vein.[14, 15] An asymmetric bilayered structure, called the ductal plate structure, then forms when a certain population of BEC precurors differentiates to BECs and a layer of hepatoblast forms above it via an unknown mechanism.[14, 15] At this point, a lumen starts to form between the layers. The cells of the first layer are polarized, displaying a higher expression of polarity markers such as E-cadherin and laminin, while hepatoblasts of the upper layer display no or little expression.[14] This reflects the asymmetrical organization of the structure. The second layer subsequently differentiates to BECs and completes the formation of a mature tubule.[14, 15]

Zebrafish biliary duct development is different than mammals in that proliferation and active remodeling drives the morphogenesis. In Lorent *et al*., zebrafish biliary duct development was characterized utilizing a new transgenic line that expresses eGFP in all cells that are responsive to Notch signaling (Tg(Tp1bglob:eGFP)).[16] These GFP-positive cells in the liver are all positive for biliary cell markers.[16] The initial premature network of BECs undergoes expansion via proliferation and morphogenesis via remodeling at the same time. A large network of BECs with functional tubules is generated.[16] While extensive proliferation of BECs is observed, it is possible that population expansion is also due to differentiation.[16] During remodeling, BECs are actively moving and rearranging. Filopodia from BECs are also actively projecting and retracting to connect with new neighbors.[16] It is unclear whether such remodeling process occurs in mammalian biliary ductal morphogenesis.

However, similar to mammals, polarization and biliary morphogenesis seem to occur in parallel. In zebrafish, as the endothelial cells invade the liver and contact one surface of hepatocytes, it signals to the hepatocytes that that surface will be the basal surface.[17] Consequently, the hepatocytes polarizes and apical proteins such as aPKC and Alcam localizes to the apical domain of the hepatocytes.[17] The apical domain defines the location of the biliary ducts.[17] It will be interesting to identify molecules involved in coordinating the two processes.

References

1. Kitajiri, S., et al., *Compartmentalization established by claudin-11-based tight junctions in stria vascularis is required for hearing through generation of endocochlear potential.* J Cell Sci, 2004. **117**(Pt 21): p. 5087-96.
2. Van Itallie, C.M. and J.M. Anderson, *Claudins and epithelial paracellular transport.* Annu Rev Physiol, 2006. **68**: p. 403-29.
3. Furuse, M. and S. Tsukita, *Claudins in occluding junctions of humans and flies.* Trends Cell Biol, 2006. **16**(4): p. 181-8.
4. Matter, K., et al., *Mammalian tight junctions in the regulation of epithelial differentiation and proliferation.* Curr Opin Cell Biol, 2005. **17**(5): p. 453-8.
5. Simon, D.B., et al., *Paracellin-1, a renal tight junction protein required for paracellular Mg2+ resorption.* Science, 1999. **285**(5424): p. 103-6.
6. Weber, S., et al., *Novel paracellin-1 mutations in 25 families with familial hypomagnesemia with hypercalciuria and nephrocalcinosis.* J Am Soc Nephrol, 2001. **12**(9): p. 1872-81.
7. Kitajiri, S.I., et al., *Expression patterns of claudins, tight junction adhesion molecules, in the inner ear.* Hear Res, 2004. **187**(1-2): p. 25-34.
8. Wilcox, E.R., et al., *Mutations in the gene encoding tight junction claudin-14 cause autosomal recessive deafness DFNB29.* Cell, 2001. **104**(1): p. 165-72.
9. Gow, A., et al., *Deafness in Claudin 11-null mice reveals the critical contribution of basal cell tight junctions to stria vascularis function.* J Neurosci, 2004. **24**(32): p. 7051-62.

10. Fujita, H., et al., *Differential expression and subcellular localization of claudin-7, -8, -12, -13, and -15 along the mouse intestine.* J Histochem Cytochem, 2006. **54**(8): p. 933-44.

11. Tamura, A., et al., *Megaintestine in claudin-15-deficient mice.* Gastroenterology, 2008. **134**(2): p. 523-34.

12. Horne-Badovinac, S., et al., *Positional cloning of heart and soul reveals multiple roles for PKC lambda in zebrafish organogenesis.* Curr Biol, 2001. **11**(19): p. 1492-502.

13. Wallace, K.N. and M. Pack, *Unique and conserved aspects of gut development in zebrafish.* Dev Biol, 2003. **255**(1): p. 12-29.

14. Antoniou, A., et al., *Intrahepatic bile ducts develop according to a new mode of tubulogenesis regulated by the transcription factor SOX9.* Gastroenterology, 2009. **136**(7): p. 2325-33.

15. Zong, Y., et al., *Notch signaling controls liver development by regulating biliary differentiation.* Development, 2009. **136**(10): p. 1727-39.

16. Lorent, K., et al., *Reiterative use of the notch signal during zebrafish intrahepatic biliary development.* Dev Dyn. **239**(3): p. 855-64.

17. Sakaguchi, T.F., et al., *Endothelial signals modulate hepatocyte apicobasal polarization in zebrafish.* Curr Biol, 2008. **18**(20): p. 1565-71.

Chapter 2:

Genetic control of single lumen formation in the zebrafish gut.

Abstract

Most organs consist of networks of interconnected tubes that serve as conduits to transport fluid and cells and act as physiological barriers between compartments. Biological tubes are assembled through very diverse developmental processes that generate structures of different shapes and sizes. Nevertheless, all biological tubes invariably possess one single lumen. The mechanisms responsible for single lumen specification are not known. Here we show that zebrafish mutants for the MODY5 and familial GCKD gene tcf2 (also known as vhnf1) fail to specify a single lumen in their gut tube and instead develop multiple lumens. We show that Tcf2 controls single lumen formation by regulating claudin15 and Na^+/K^+-ATPase expression. Our in vivo and in vitro results indicate that Claudin15 functions in paracellular ion transport to specify single lumen formation. This work shows that single lumen formation is genetically controlled and appears to be driven by the accumulation of fluid.

Introduction

Many organs such as the lung, kidney, gut, and mammary gland have tubular structures that serve an essential function of transporting vital substances. Tubes of various organs develop through different morphological processes to generate different sized and shaped tubes.[1] There are 5 such processes described.[1] The neural tube uses a process called wrapping in which an epithelial sheet bends and invaginates such that the ends meet to form a tube. During lung morphogenesis, new tubes are generated when epithelial cells branch out orthogonal to the existing tube in a process called budding. In both wrapping and budding, the new tube is formed from an existing polarized epithelium. Thinner tubes such as those of the capillaries utilize a cell hollowing mechanism. Tubes generated with this method involve only one cell where intracellular vesicles with luminal proteins fuse and expand to create a lumen within the cell. The last two processes, cavitation and cord hollowing, start with an initial solid rod of cells multiple layers thick. During cavitation, cells in the middle of the rod undergo apoptosis to clear way for a lumen. During cord hollowing mechanism, cells rearrange themselves into a radial pattern and a lumen is formed in the middle. Cell death is not involved in cord hollowing. Regardless of how the tubes are formed, the resulting tubes all have the unique characteristics of being lined with polarized epithelial cells and having a single lumen.

The single layer of epithelial cells that line each tube acts as a barrier between the organism and the outside environment. Epithelial cells are polarized with free apical membrane domains that face the lumen, lateral domains that interact with neighboring cells, and basal domains that attach to the extracellular matrix. Proper polarization is

important for regulated processes such as directional gas and nutrient exchange. Furthermore, *in vitro* and *in vivo* studies have shown that epithelial cells polarization and tube formation is intimately linked.[2, 3]

All tubes have single lumen to facilitate fluid transport, including the gut tube. It has been shown that apical membrane biogenesis and vesicle fusion are important for lumen formation while secretion plays a role in tubular growth.[1] In MDCK cells, cytosolic vacuolar apical compartments containing apical and luminal proteins exocytose to the region of cell-cell contact to create an apical surface and luminal space.[4, 5] Apical membrane biogenesis have also been shown in Drosophila trachea to regulate tube growth.[6] Cell proliferation does not seem to be involved since mutations in cell cycle regulators do not affect tube size.[6] Subsequent to apical membrane biogenesis, secretion of liquids into the lumen drives its expansion.[7] As each epithelial cell in the tube undergoes genetic programs for apical membrane biogenesis, how these cells coordinate and the cellular processes that specify a single lumen is not known.

Analysis of some zebrafish polarity mutants revealed defects in polarity results in the formation of multiple lumens in the gut.[8](Appendix 1) The zebrafish gut provides an excellent and accessible model to study tubulogenesis *in vivo*. The primitive zebrafish gut tube is a solid rod of unpolarized cells. To form a functional tube, a lumen is formed between cells of a cylindrical cord via the cord hollowing mechanism. Active, cleaved form of caspase-3 were not found in the gut during lumen formation suggesting that apoptosis is not involved.[9] In a cross section view, the intestinal tube is initially a collection of endodermal cells that are not polarized. Actin foci at points of cell-cell contact are observed. The cells then undergo rearrangement to organize into a radial

pattern. The actin foci appear to cluster together to a single focal point in the middle of the rod where it marks the site of future lumen formation[8]. In subsequent studies, we observed restricted localization of ZO-1 and cadherins to suggest that cells are polarizing as they rearrange (Appendix 1). In the polarity mutants, there appear to be inefficiency in the clustering of the actin foci which results in a failure to form a single lumen.

In this study, we observed that mutation in the homeobox gene Tcf2 also causes a multiple lumen phenotype in the zebrafish gut tube. Tcf2 is associated with MODY5(maturity-onset diabetes of the young, type V) and familial GCKD (glomerulocystic kidney disease). Zebrafish *tcf2* mutants exhibit defects in liver and pancreas development and most notably, cysts form in the pronephros.[10] Our study indicates that Tcf2 transcriptionally regulate expression of claudin15 and Na^{+}/K^{+}-ATPase. Together, these proteins work to establish the proper osmotic gradient to ensure formation of a single lumen in the gut tube.

Results and Discussion

The zebrafish gut tube originates from a solid rod of endodermal cells that forms a lumen as the cells polarize, but without apoptosis[9, 11, 12]. Tcf2 has been shown to be required for endoderm differentiation in mammals[13], and zebrafish *tcf2* mutants have defects in gut, liver and pancreas morphogenesis[10]. To explore the role of *tcf2* in zebrafish gut tube formation we used the null insertional allele $tcf2^{2169}$ [10]and analysed gut morphology 72 hours post fertilization (h.p.f.) by confocal microscopy. In transverse section, some $tcf2^{2169}$ mutants showed pronephric cysts, as reported previously[10]; most strikingly, however, some mutants presented multiple lumens in the intestinal bulb, the region of the zebrafish intestine that acts as a stomach (Fig. 2.1a, top). These phenotypes could be found together or separately and are therefore most probably independent from each other. Using a membrane-bound green fluorescent protein we observed lumens that were open through long stretches and also others that were only a few cells long (see Supplementary Information, Fig. S2.1). We did not observe multiple lumens in the posterior gut, a part of the tube that has fewer cells (not shown). To determine whether tight and adherens junctions were properly formed in $tcf2^{2169}$ mutant gut epithelial cells, we stained transverse sections with antibodies against cadherin and the tight junction marker zonula occludens protein-1 (ZO-1). At 72 h.p.f., about half of the mutant larvae (47.5%, $n = 101$) presented multiple gut lumens in which both markers were localized correctly. A fraction of the mutants (17.8%) did not show a discernible lumen and presented an unpolarized distribution of cadherin (Fig. 2.1a). In contrast, we could not find any multiple lumen gut in wild-type (WT) larvae at 72 h.p.f. ($n = 250$). To understand normal gut morphogenesis we examined WT embryos at different time points.

At about 36 h.p.f., some cells of the endodermal rod expressed the junctional marker ZO-1 and showed some degree of polarization, but no obvious luminal structure could be observed. Then, at about 43 h.p.f., we observed multiple small lumens marked by ZO-1 (Fig. 2.1b), and apparent as small clear spaces by transmission electron microscopy (see Supplementary Information, Fig. S2.1). These multiple lumens coalesced into a single larger lumen by 48 h.p.f. (Fig. 2.1b). At 96 h.p.f., the multiple lumen phenotype was still present in *tcf2*^{2169} mutants (Fig. 2.1a), suggesting that this phenotype represents an arrest in the lumen formation process. These data indicate that single lumen formation in the zebrafish intestinal bulb is a very efficient process that involves the coalescence of multiple small lumens and is controlled by the transcription factor Tcf2.

Next we analysed potential downstream effectors of Tcf2. The atypical protein kinase C λ (aPKC-λ, also known as prkci) mutant *heart and soul* (*has*) was previously shown to develop multiple lumens in the gut[8]. However, the penetrance of this phenotype is much lower in *has* (7.8%, n = 152) than in *tcf2*^{2169} mutant larvae (see Supplementary Information, Fig. S2.2a). In addition, aPKC-λ expression levels did not seem to be affected in *tcf2*^{2169} mutants (see Supplementary Information, Fig. S2.2b), suggesting that aPKC-λ is not an effector of Tcf2 in gut lumen formation. Because apical membrane formation has been implicated in tubulogenesis and lumen expansion in *Drosophila*[1], we tested whether apical membrane formation was affected in *tcf2*^{2169} mutant larvae. We first examined the localization of aPKC-λ and the apical antigen 4e8[14] and found that they were expressed and localized properly in *tcf2*^{2169} mutant larvae (see Supplementary Information, Fig. S2.2b,c). Next we examined two mutants that had previously been shown to be affected in different aspects of apical membrane

biogenesis in the retinal epithelium. Both *mosaic eyes* (*moe*, also known as *epp41l5*)[15] and *nagie oko* (*nok*, also known as *mpp5*)[16] mutants showed small gut lumens but did not present a multiple lumen phenotype (see Supplementary Information, Fig. S2.2d,e). These data suggest that apical membrane expansion does not have a major role in gut lumen coalescence.

To identify Tcf2-regulated factors involved in single lumen formation we used DNA microarray analyses to find genes downregulated in *tcf2*^{2169}mutants compared with WT. Consistent with previous work[10] was our observation, among the genes regulated by Tcf2, of several enzyme-coding genes specific to liver and pancreas, including a liver fatty-acid-binding-protein gene (*lfabp10*) whose expression was decreased 20-fold. We confirmed these data by looking at the expression of DsRed driven by the *lfabp* promoter[17] (*lfabp:DsRed*) in WT and *tcf2*^{2169} mutant larvae (Fig. 2.2a). When we examined genes that showed a more than twofold decrease in expression levels, we found that *claudin15* (*cldn15*) was downregulated 5.3-fold in *tcf2*^{2169} mutants compared with WT (for a partial list of genes downregulated in *tcf2*^{2169} mutant larvae see Supplementary Information, Table S1). To check whether *cldn15* expression is indeed regulated by Tcf2 we performed *in situ* hybridization (ISH) analysis. At 72 h.p.f., we could detect *cldn15* expression in the gut of WT but not *tcf2*^{2169} mutant larvae (Fig. 2.2b). Next we examined *cldn15* expression during WT development. We detected expression in the midgut at about 36 h.p.f. that became stronger and extended towards the posterior gut later in development (Fig. 2.2c). At 72 h.p.f., *cldn15* expression could also be detected in the pronephros and pancreas. These data show that *cldn15* is expressed in the gut under the control of Tcf2 at the time when lumen coalescence takes place.

To test whether Cldn15 is required for single lumen formation we knocked down its expression by using a morpholino directed against the translation initiation site. Most (more than 80%) Cldn15 morphants phenocopied *tcf2*^{2169} mutants (Fig. 2.2d). When we analysed gut lumen formation in Cldn15 morphants, we found that a significant fraction (34.7%, $n = 78$) showed a multiple lumen phenotype in the intestinal bulb that did not affect the localization of cadherin or ZO-1 (Fig. 2.2e). The phenotype of Cldn15 morphants was specific to the gut, because the pronephric and neural tubes were not affected (Fig. 2.2e). To confirm that Cldn15 was indeed knocked down we analysed Cldn15 expression and localization by using an antibody generated against human Cldn10, a protein that shares significant homology to zebrafish Cldn15[18]. This antibody specifically recognized zebrafish Cldn15 transfected into HEK293 cells (see Supplementary Information, Fig. S2.3a,b), a human cell line that does not express claudins. In WT zebrafish larvae, this antibody stained tight junctions in the gut and pronephros, where it colocalized with ZO-1. It also stained the notochord where colocalization with ZO-1 was only partial (Fig. 2.2f). The notochord signal most probably corresponds to another antigen, perhaps another claudin, that crossreacts with the antibody, because we did not detect *cldn15* expression in the notochord. Importantly, the staining was absent in the gut of Cldn15 morphants (Fig. 2.2f), indicating that Cldn15 was effectively knocked down by the morpholino. The multiple lumen phenotype observed in Cldn15 morphants seems to be specific because larvae in which the tight-junction protein occludin was knocked down did not show any defects in gut lumen formation ($n = 35$) (see Supplementary Information, Fig. S2.3c,d). Taken together, these

data strongly suggest that Tcf2 controls lumen coalescence in the zebrafish gut, at least in part through Cldn15.

Recently, the *Drosophila* claudin mutants *sinuous*[19] and *megatrachea*[20] were shown to have tracheal tube defects. In both mutants, assembly of the septate junction—the functional equivalent of the vertebrate tight junction—and the barrier function in tracheal epithelial cells was affected. To test whether the barrier function was compromised in *tcf2*^{2169} mutants, we injected the yolk of 72 h.p.f. WT and mutant larvae with two tracers that had been previously used to assay the barrier function in vertebrates, rhodamine-dextran of relative molecular mass 10,000 (M_r 10K) and a biotinylation reagent (M_r 443)[21], to determine whether they reached the apical side of gut epithelial cells. In WT and *tcf2*^{2169} mutant larvae, both tracers reached the basolateral surface of gut epithelial cells and marked the entire lateral surface but could not be detected on the apical side (Fig. 2.3a). This experiment, together with the normal localization of ZO-1, indicates that in *tcf2*^{2169} mutants the tight junctions in the gut are still present and able to function as barriers for molecules of M_r 443 or more, probably as a result of the presence of other claudins that are not regulated by Tcf2 (data not shown).

Claudins have also been shown to form paracellular pores that allow the selective passage of ions across epithelia down an electrochemical gradient formed by the Na^+/K^+-ATPase[22, 23]. Mutations in *CLDN16* cause familial hypomagnesaemia in humans[24]. When transfected into LLC-PK1 epithelial cells, CLDN16 increases paracellular permeability to Na^+, suggesting that the lack of $Mg2^+$ reabsorption probably resulted from a dissipation of the transepithelial potential[25]. Paracellular ion permeability can be estimated by measuring the transepithelial electrical resistance (TER). TER is high in

'tight' epithelia and low in 'leaky' epithelia[23, 26, 27]. Expression of different claudins in various cell lines can either increase or decrease their TER; this measure has therefore been used to determine the ion pore-forming properties of claudins[26, 28]. We hypothesized that Cldn15 might form a paracellular pore that would allow the movement of ions and fluid into the gut lumen; in turn, fluid accumulation would provide the force to drive lumen coalescence. To test this hypothesis, we generated cell lines stably expressing untagged Cldn15. When expressed in MDCKII or LLC-PK1 cells, Cldn15 was efficiently targeted to the tight junction and colocalized with ZO-1 (Fig. 2.3b). Although Cldn15 expression in the low TER MDCKII background did not change the TER significantly ($n = 6$), it markedly decreased (sevenfold, $n = 6$) the TER in tighter LLC-PK1 cells compared with control cells (transfected with empty vector) (Fig. 2.3c), indicating that Cldn15 can form ion-permeable pores in epithelial tight junctions. Importantly, even though the TER was reduced, the epithelial sheet remained tight and did not allow transepithelial passage of two different tracers, M_r 10K rhodamine-dextran and fluorescein isothiocyanate (FITC)-inulin (M_r 2K–5K) (Fig. 2.3d).

To test the role of fluid accumulation, as well as of Cldn15, during lumen formation, we optimized an *in vitro* lumen formation assay by using epithelial cysts cultured over a thin layer of Matrigel. We initially used the LLC-PK1 cell lines that we generated; however, these cells did not form cysts (data not shown). To circumvent this limitation we turned to MDCKC7 cells, which display a very high TER[29]. Stable lines expressing Cldn15 (Fig. 2.4a) showed a very drastic decrease in TER compared with control cells (Fig. 2.4b), confirming the results obtained with LLC-PK1 cells. We next cultured these cells in Matrigel to assess the effect of Cldn15 on lumen formation. After 4

days in culture, control MDCKC7 cells formed single lumen cysts, somewhat inefficiently (only 44% single lumen), that were mostly (92%) smaller than 50 μm in lumen diameter; only 8% had a lumen that was 50–100 μm wide. On expression of Cldn15, the fraction of cysts with a single lumen increased by more than 60% (P = 0.0002). This effect was accompanied by a significant increase in lumen size, with a large fraction of cysts (49.3%) having a lumen 50–100 μm wide and a significant fraction (12.7%) being larger than 100 μm (Fig. 2.4d, left panels). Next, to test the role of fluid accumulation on single lumen formation we treated cysts with forskolin and/or ouabain. Forskolin has been shown to promote fluid accumulation and cyst lumen expansion, mainly through the kinase-dependent activation of apical chloride channels[30, 31]. In contrast, inhibition of the Na^+/K^+-ATPase with the glycoside ouabain disrupts the formation of the electrochemical gradient necessary to drive paracellular and transcellular ion transport, thus producing the opposite effect (a diagram is shown in Fig. 2.4c). The addition of forskolin (10 μM) not only led to a marked increase in cyst lumen size as shown before with other cell types[31], but also increased by more than 50% the fraction of MDCKC7 cysts with a single lumen (P = 0.0095). Forskolin was significantly more effective in cells expressing Cldn15 (P = 0.022 compared with MDCKC7 plus forskolin; P = 0.0065 compared with Cldn15 control), indicating a synergy between paracellular and transcellular ion transport. Conversely, ouabain (0.1 μM) blocked single lumen formation and expansion (all lumens were smaller than 50 μm) in all cases (Fig. 2.4c). These data show a direct role for Cldn15 in single lumen formation and lumen size control, and they illustrate the role of fluid accumulation in this process *in vitro*. To investigate whether this mechanism also operates *in vivo*, we injected the yolk of 30 h.p.f.

WT embryos with small amounts of ouabain or forskolin and analysed lumen formation in the gut as before. Injection of forskolin led to a significant enlargment of the gut lumen. In contrast, injection of ouabain produced a dose-dependent multiple lumen phenotype (26% multiple lumen (n = 46) with 3 nl of 100 μM ouabain; 50% (n = 26) with 3 nl of 200 μM ouabain) that was identical to that in *tcf2*^{2169} mutant larvae (Fig. 2.5a). We next tried to rescue *tcf2*^{2169} mutants by injecting forskolin. Because forskolin had no effect on *tcf2*^{2169} mutants (Fig. 2.5a), we checked expression of the Na^+/K^+-ATPase. Staining with antibodies revealed that although the protein was expressed at wild-type or higher levels in the pronephros and neural tube it was absent from the gut of *tcf2*^{2169} mutants, indicating that Tcf2 also controls Na^+/K^+-ATPase expression in the gut (Fig. 2.5b).

Here we have shown that the formation of a single lumen, a defining characteristic of all biological tubes, is genetically controlled. Our data demonstrate that regulation of Cldn15 and Na^+/K^+-ATPase expression by Tcf2 is required for single lumen specification in the intestinal bulb of the zebrafish gut. The posterior gut and pronephros, which also express Cldn15 under the control of Tcf2, did not show defects in lumen formation. This difference can be explained by the fact that in these tubes all cells are in close proximity and are therefore able to establish continuous tight junctions before the lumen opens.

Claudins have been shown to form Ca^{2+}-independent adhesions when transfected into fibroblasts, through the interaction of the extracellular domains of molecules present in adjacent cells[32]. We were able to recreate this phenomenon in HEK293 cells expressing zebrafish Cldn15 (see Supplementary Information, Fig. S2.3). However, although it is possible that claudin-based cell–cell adhesion may contribute to the process,

it is unlikely that protein–protein interactions alone would be able to drive the coalescence of lumens that may be several cells apart. We propose that the electrochemical gradient generated by the Na^+/K^+-ATPase drives vectorial ion movement through Cldn15-based paracellular pores. Asymmetric ion distribution would produce luminal fluid accumulation that would lead to the expansion of multiple small lumens and provide the force for their coalescence (Fig. 2.5c).

To maintain an open luminal space, all biological tubes must be filled with liquid, gas or other materials at all times. Recent work in *Drosophila* has revealed a role for apical matrix deposition during lumen formation in the retina[33] and tracheal system[34, 35]. In both cases it seems that the apical matrix functions as a scaffold to support the initial stages of lumen formation. In vertebrates, fluid accumulation has been implicated in neural tube expansion[36]. Our work suggests that fluid accumulation could simultaneously provide the driving force for lumen expansion and ensure that a single lumen is formed.

Materials and Methods

Animals. AB wild-type and mutant alleles *tcf2*^{2169}, *has*^{m567}, *moe*^{b781} and *nok*^{m520} were maintained as described previously[17, 21, 24, 25]. The *tcf2*^{2169} mutation was crossed into the *lfabp:DsRed* transgenic line[37].

Cells and antibodies. MDCKII cells were grown in MEM medium supplemented with 5% fetal bovine serum. LLC-PKI cells were grown in M-199 medium supplemented with 3% fetal bovine serum. HEK293 cells were grown in DMEM medium supplemented with 10% fetal bovine serum. Antibodies against human ZO-1, Cldn10 and occludin were from Zymed (Carlsbad, CA, USA**)**. Rabbit anti-pan-cadherin was from Sigma, and rabbit anti-aPKC was from Santa Cruz (Santa Cruz, CA, USA). Mouse monoclonal antibody 4e8[23] was provided by J. Lewis (Cancer ResearchUK London Institute, London, UK). Alexa647-phalloidin was from Molecular Probes.

Expression vectors and stable cell lines. To establish stable cell lines expressing zebrafish Cldn15 (accession number NM_200404) the full-length cDNA was amplified by PCR from a full-length cDNA clone (catalogue number 6791205; Open Biosystems, Huntsville, AL, USA) and inserted into the mammalian expression vector pCDNA3 (Invitrogen, Carlsbad, CA, USA). Cells were transfected with Lipofectamine 2000 (Promega, Madison, WI, USA). MDCKII and LLC-PKI cells expressing Cldn15 were selected in medium containing 500 and 750 μm ml^{-1}
G418, respectively.

Morpholino knockdown. The Cldn15 (MORPH1234, 5′-ATGATCGGATCCATTGTAGCTGC AG-3′; Open Biosystems) and occludin a (MORPH1463, 5′-GACTCCCGATGTGCTTCGACG ACA-3′; Open Biosystems) morpholinos were targeted against the translational start.

***In situ* hybridization.** Whole-mount *in situ* hybridizations were performed as described previously[14]. The *cldn15* (accession number NM_200404) *in situ* probe corresponds to nucleotides 589–1158. The *in situ* construct was cloned into pGEMT-easy (Promega) with *Bam* HI/*Xho* I, linearized with *Xho* I and transcribed with T7 RNA polymerase.

Immunohistochemistry. For pan-cadherin and F-actin staining, larvae were fixed in 4% formaldehyde in egg water at 4 °C overnight. The fixed larvae were washed in PBS and embedded in 4% low-melt agarose in PBS. Transverse sections 250 μm thick were obtained with a vibratome (Leica, Bannockburn, IL, USA). For Cldn15 and occludin stainings, larvae were fixed in trichloroacetic acid for 1 h on ice.

Immunofluorescence. After 7 days of culture on transwell filters, cells were fixed with 10% trichloroacetic acid and stained as described previously[8].

Confocal imaging. Confocal imaging was performed with a Zeiss LSM510 laserscaning microscope. Images were analysed with LSM software (Zeiss, Thornwood, NY, USA) and Photoshop 7.0 (Adobe).

***In vivo* paracellular tracer flux assay.** Larvae at 72 h.p.f. were anaesthetized in 0.1 mg ml^{-1} tricaine (Sigma, St Louis, MO, USA) and injected into the yolk with 10–20 nl of 1% rhodamine-dextran (*M*r 10K; Molecular Probes, Carlsbad, CA, USA) and 10 mg ml^{-1} EZ-Link sulpho-NHS-biotin (Pierce, Rockford, IL, USA) in 0.2 M KCl. After incubation for 2 h at 28 °C, larvae were fixed and processed for immunohistochemistry. Biotin was detected with Alexa488-streptavidin.

Measurement of TER and paracellular tracer flux. After 7 days of culture on transwell filters, TER was measured directly in culture medium at 24 °C with a Millicell-ERS epithelial voltohmmeter (Millipore, Billerica, MA, USA). Paracellular tracer flux was measured with 1 mg ml^{-1} rhodamine-dextran (*M*r10K) and FITC-inulin (Sigma) as described previously[8].

Lumen formation in epithelial cysts. Control MDCKC7 and Cldn15-expressing cells were grown on DMEM (H21) medium supplemented with 2% Matrigel over a thin layer of 100% Matrigel for 2 days, to allow cyst formation. Then the medium was replaced with fresh medium containing 2% Matrigel and dimethylsulphoxide (DMSO; control), forskolin (10 μM) or ouabain (0.1 μM) and cells were cultured for a further 2 days.

Gene accession numbers. *lfabp10* (NM_152960), *cldn15* (NM_200404), *occluding a* (NM_21832).

References

1. Lubarsky, B. and M.A. Krasnow, *Tube morphogenesis: making and shaping biological tubes.* Cell, 2003. **112**(1): p. 19-28.
2. O'Brien, L.E., M.M. Zegers, and K.E. Mostov, *Opinion: Building epithelial architecture: insights from three-dimensional culture models.* Nat Rev Mol Cell Biol, 2002. **3**(7): p. 531-7.
3. Hogan, B.L. and P.A. Kolodziej, *Organogenesis: molecular mechanisms of tubulogenesis.* Nat Rev Genet, 2002. **3**(7): p. 513-23.
4. Vega-Salas, D.E., P.J. Salas, and E. Rodriguez-Boulan, *Modulation of the expression of an apical plasma membrane protein of Madin-Darby canine kidney epithelial cells: cell-cell interactions control the appearance of a novel intracellular storage compartment.* J Cell Biol, 1987. **104**(5): p. 1249-59.
5. Vega-Salas, D.E., P.J. Salas, and E. Rodriguez-Boulan, *Exocytosis of vacuolar apical compartment (VAC): a cell-cell contact controlled mechanism for the establishment of the apical plasma membrane domain in epithelial cells.* J Cell Biol, 1988. **107**(5): p. 1717-28.
6. Beitel, G.J. and M.A. Krasnow, *Genetic control of epithelial tube size in the Drosophila tracheal system.* Development, 2000. **127**(15): p. 3271-82.
7. Hooper, S.B. and R. Harding, *Fetal lung liquid: a major determinant of the growth and functional development of the fetal lung.* Clin Exp Pharmacol Physiol, 1995. **22**(4): p. 235-47.

8. Horne-Badovinac, S., et al., *Positional cloning of heart and soul reveals multiple roles for PKC lambda in zebrafish organogenesis.* Curr Biol, 2001. **11**(19): p. 1492-502.

9. Ng, A.N., et al., *Formation of the digestive system in zebrafish: III. Intestinal epithelium morphogenesis.* Dev Biol, 2005. **286**(1): p. 114-35.

10. Sun, Z. and N. Hopkins, *vhnf1, the MODY5 and familial GCKD-associated gene, regulates regional specification of the zebrafish gut, pronephros, and hindbrain.* Genes Dev, 2001. **15**(23): p. 3217-29.

11. Ober, E.A., H.A. Field, and D.Y. Stainier, *From endoderm formation to liver and pancreas development in zebrafish.* Mech Dev, 2003. **120**(1): p. 5-18.

12. Wallace, K.N. and M. Pack, *Unique and conserved aspects of gut development in zebrafish.* Dev Biol, 2003. **255**(1): p. 12-29.

13. Barbacci, E., et al., *Variant hepatocyte nuclear factor 1 is required for visceral endoderm specification.* Development, 1999. **126**(21): p. 4795-805.

14. Crosnier, C., et al., *Delta-Notch signalling controls commitment to a secretory fate in the zebrafish intestine.* Development, 2005. **132**(5): p. 1093-104.

15. Jensen, A.M. and M. Westerfield, *Zebrafish mosaic eyes is a novel FERM protein required for retinal lamination and retinal pigmented epithelial tight junction formation.* Curr Biol, 2004. **14**(8): p. 711-7.

16. Wei, X. and J. Malicki, *nagie oko, encoding a MAGUK-family protein, is essential for cellular patterning of the retina.* Nat Genet, 2002. **31**(2): p. 150-7.

17. Her, G.M., Y.H. Yeh, and J.L. Wu, *435-bp liver regulatory sequence in the liver fatty acid binding protein (L-FABP) gene is sufficient to modulate liver regional expression in transgenic zebrafish.* Dev Dyn, 2003. **227**(3): p. 347-56.

18. Loh, Y.H., et al., *Extensive expansion of the claudin gene family in the teleost fish, Fugu rubripes.* Genome Res, 2004. **14**(7): p. 1248-57.

19. Wu, V.M., et al., *Sinuous is a Drosophila claudin required for septate junction organization and epithelial tube size control.* J Cell Biol, 2004. **164**(2): p. 313-23.

20. Behr, M., D. Riedel, and R. Schuh, *The claudin-like megatrachea is essential in septate junctions for the epithelial barrier function in Drosophila.* Dev Cell, 2003. **5**(4): p. 611-20.

21. Nitta, T., et al., *Size-selective loosening of the blood-brain barrier in claudin-5-deficient mice.* J Cell Biol, 2003. **161**(3): p. 653-60.

22. Tsukita, S. and M. Furuse, *Pores in the wall: claudins constitute tight junction strands containing aqueous pores.* J Cell Biol, 2000. **149**(1): p. 13-6.

23. Van Itallie, C.M. and J.M. Anderson, *Claudins and epithelial paracellular transport.* Annu Rev Physiol, 2006. **68**: p. 403-29.

24. Simon, D.B., et al., *Paracellin-1, a renal tight junction protein required for paracellular Mg2+ resorption.* Science, 1999. **285**(5424): p. 103-6.

25. Hou, J., D.L. Paul, and D.A. Goodenough, *Paracellin-1 and the modulation of ion selectivity of tight junctions.* J Cell Sci, 2005. **118**(Pt 21): p. 5109-18.

26. Furuse, M., et al., *Conversion of zonulae occludentes from tight to leaky strand type by introducing claudin-2 into Madin-Darby canine kidney I cells.* J Cell Biol, 2001. **153**(2): p. 263-72.

27. Matter, K. and M.S. Balda, *Functional analysis of tight junctions.* Methods, 2003. **30**(3): p. 228-34.

28. Van Itallie, C.M. and J.M. Anderson, *The role of claudins in determining paracellular charge selectivity.* Proc Am Thorac Soc, 2004. **1**(1): p. 38-41.

29. Gekle, M., et al., *Characterization of two MDCK-cell subtypes as a model system to study principal cell and intercalated cell properties.* Pflugers Arch, 1994. **428**(2): p. 157-62.

30. Grantham, J.J., et al., *In vitro fluid secretion by epithelium from polycystic kidneys.* J Clin Invest, 1995. **95**(1): p. 195-202.

31. Li, H., I.A. Findlay, and D.N. Sheppard, *The relationship between cell proliferation, Cl- secretion, and renal cyst growth: a study using CFTR inhibitors.* Kidney Int, 2004. **66**(5): p. 1926-38.

32. Kubota, K., et al., *Ca(2+)-independent cell-adhesion activity of claudins, a family of integral membrane proteins localized at tight junctions.* Curr Biol, 1999. **9**(18): p. 1035-8.

33. Husain, N., et al., *The agrin/perlecan-related protein eyes shut is essential for epithelial lumen formation in the Drosophila retina.* Dev Cell, 2006. **11**(4): p. 483-93.

34. Devine, W.P., et al., *Requirement for chitin biosynthesis in epithelial tube morphogenesis.* Proc Natl Acad Sci U S A, 2005. **102**(47): p. 17014-9.

35. Tonning, A., et al., *A transient luminal chitinous matrix is required to model epithelial tube diameter in the Drosophila trachea.* Dev Cell, 2005. **9**(3): p. 423-30.

36. Lowery, L.A. and H. Sive, *Initial formation of zebrafish brain ventricles occurs independently of circulation and requires the nagie oko and snakehead/atp1a1a.1 gene products.* Development, 2005. **132**(9): p. 2057-67.

37. Dong, P.D., et al., *Fgf10 regulates hepatopancreatic ductal system patterning and differentiation.* Nat Genet, 2007. **39**(3): p. 397-402.

Figure Legends

Figure 2.1 Gut lumen formation in WT and *tcf2*^{2169} mutant larvae.

a, Top: confocal images of transverse sections of 72 h.p.f. WT and *tcf2*^{2169} mutant larvae stained with rhodamine-phalloidin to visualize F-actin. Multiple lumens are present in the gut of *tcf2*^{2169} mutant larvae at 72 h.p.f. The arrows point to the gut lumens and the arrowheads to the pronephric duct lumen. k.c., kidney cyst. Middle: confocal images of transverse sections of 72 h.p.f. WT and *tcf2*^{2169} mutant larvae stained for pan-cadherin (green), ZO-1 (red) and alexa647-phalloidin (blue). Bottom: 96 h.p.f. WT and *tcf2*^{2169} mutant larvae processed as in the middle panel.

b, Confocal images of transverse sections of WT larvae collected at the indicated time points, stained for F-actin (green, false colour) and ZO-1 (red). At 43 h.p.f. multiple lumens can be seen (arrows). Scale bars, 20 μm.

Figure 2.2 Tcf2 controls Cldn15 expression in the gut; Cldn15 knockdown larvae have multiple gut lumens.

a, lfabp:DsRed is expressed at 72 h.p.f. in the liver (L) of WT larvae but undetectable in *tcf2*^{2169} mutant larvae. Larvae were fixed, sectioned and stained for cadherin (green), ZO-1 (red) and F-actin (blue). Scale bar, 20 μm.

b, *cldn15 in situ* hybridization. *cldn15* is expressed in the gut of WT larvae but not in that of *tcf2*^{2169} mutant larvae at 72 h.p.f.

c, Time course of *cldn15* expression in WT larvae.

d, Whole-body phenotype of *tcf2*^{2169} mutant larvae and Cldn15 morphants at 72 h.p.f.

e, Confocal images of transverse sections of control (uninjected) larvae and Cldn15 morphants stained for cadherin (green) and ZO-1 (red). Arrows points to the gut lumens.

f, Cldn15 (green) colocalizes with ZO-1 (red) at the tight junction in WT larvae. Expression of Cldn15 is abolished in the morphants. The antibody used for Cldn15 also reacts with an antigen expressed in the notochord (Ntc). Scale bars, 20 μm.

Figure 2.3 Cldn15 forms a paracellular ion pore.

a, The epithelial barrier remains functional in *tcf2*^{2169} mutant larvae. Rhodamine-dextran (M_r 10K) and the biotinylation reagent sulpho-NHS-biotin (S-NHS-biotin) were injected into the yolk of 72 h.p.f. WT and *tcf2*^{2169} mutant larvae. After 2 h, larvae were fixed and the distribution of the tracers was examined by confocal microscopy. Green, S-NHS-biotin; red, rhodamine-dextran; blue, F-actin. Scale bar, 20 μm.

b, Cldn15 (green) colocalizes with ZO-1 (red) in cell lines stably expressing Cldn15. Scale bar, 10 μm.

c, Stable Cldn15 expression (filled bars) reduces the TER in LLC-PK1 cells but not in MDCKII cells (n = 6) compared with control cells (open bars), which were transfected with an empty vector. Similar results were obtained with two independent clones for each cell line (only one is shown for each). Error bars indicate s.d.

d, Epithelial sheets retained barrier function. Diffusion of fluorescent tracers (rhodamine-dextran (M_r 10K) and FITC-inulin) was not affected by the expression of Cldn15. Cells incubated in buffer without Ca^{2+}, a treatment used to open the junctions, were used as a reference.

Figure 2.4 Cldn15 promotes single lumen formation through a fluid-driven mechanism.

a, Cldn15 (green) colocalizes with ZO-1 (red) in MDCKC7 cells stably expressing Cldn15. Scale bar, 10 μm.

b, Stable Cldn15 expression reduces the TER in MDCKC7 cells compared with that in control cells, which were transfected with an empty vector (n = 4). Diffusion of fluorescent tracers (rhodamine-dextran (M_r 10K) and FITC-inulin) was not affected by the expression of Cldn15 (not shown).

c, Simplified scheme of ion and water transport through the transcellular and paracellular routes. Forskolin activates apical chloride secretion and fluid accumulation, whereas ouabain inhibits the Na^+/K^+-ATPase and disrupts electrochemical gradient formation. TJ, tight junction.

d, Lumen formation in cysts. Control MDCKC7 cells or Cldn15-expressing cells were grown for 2 days over a thin layer of Matrigel to allow cyst formation. The medium was then replaced with fresh medium containing DMSO (control), forskolin (10 μM) or ouabain (0.1 μM) and cells were cultured for a further 2 days. Cysts were stained for F-actin (red), ZO-1 (green) and β-catenin (blue) and examined by confocal microscopy. Scale bar, 20 μm.

e, Quantification of three independent experiments shown in **d**. Filled bars, Cldn15-expressing cells; open bars, control cells. Error bars indicate s.d. (from left to right, n = 312, 325, 351, 327, 305, 310, 321 and 338).

Figure 2.5 Disruption of the Na^+/K^+-ATPase-dependent electrochemical gradient blocks lumen coalescence.

a, Top: confocal images of transverse sections of 72 h.p.f. WT larvae injected at 30 h.p.f. in yolk with 3 nl of ouabain (200 μM) or forskolin (10 μM) stained for pancadherin (green), ZO-1 (red) and Alexa647-phalloidin (blue). Bottom: *tcf2*^{2169} mutant larvae injected with DMSO (control) or forskolin as indicated above. The arrows point to the gut lumen. Scale bars, 20 μm.

b, Tcf2 controls expression of the Na^+/K^+-ATPase in the zebrafish gut. Na^+/K^+-ATPase is shown in red and aPKC in green. Scale bar, 20 μm.

c, Diagram of Tcf2-controlled lumen coalescence.

Supplementary Figure 2.1

a, Imaging of multiple gut lumens in *tcf2*^{2169}mutant larvae. One cell stage WT and *tcf2*^{2169} mutant embryos were injected with RNA encoding a membrane bound GFP. At 72 h.p.f. *tcf2*^{2169} mutant larvae were sorted and fixed. Serial 3 μm confocal optical sections were captured from rhodamine phalloidin stained transverse sections around the intestinal bulb. The arrow points to a small lumen that opened and closed within a 20μm interval.

b, Transmission electron micrograph of a 43 hpf WT gut in cross section. L marks nascent lumens, N=nucleus, mv=microvilli. Scale bar is 0.4 μm.

Supplementary Figure 2.2. Apical membrane formation and gut lumen specification.

a, 72 hpf WT and *has*^{m567} mutant larvae carrying the gutGFP transgene were stained for ZO-1 (red). The arrows point to the gut lumen.

b, aPKC (green) staining in 72 hpf WT and *tcf2*^{2169} mutant larvae. F-actin is shown in red. The arrows point to the gut lumen.

c, Apical antigen 4e8 (green) staining in 72 hpf WT and *tcf2*^{2169} mutant larvae. F-actin is shown in red.

d, 72 hpf Tg(gutGFP) (green) WT and *nok* (*mpp5)* mutant larvae stained for ZO-1 (red). Single lumen formation is not affected in *nok* mutants.

e, 72 hpf WT and *moe* (*epb41l5*) mutant larvae stained for ZO-1 (red), pan-Cadherin (green) and f-actin (blue). Single lumen formation is not affected in *moe* mutants.

Supplementary Figure 2.3.

a, Cldn15-GFP is recruited to cell-cell junctions in pairs of transiently transfected HEK293 cells. F-actin is shown in blue.

b, anti-human Cldn10 specifically recognizes zebrafish Cldn15 (green) transiently expressed in HEK293 cells. Nuclei are shown in blue (topro).

c, Occludin knockdown does not affect single lumen formation in the gut. WT embryos were injected with a morpholino against Occludin and stained for f-actin (red) and nuclei (blue). None of the morphants (n=35) showed lumen formation defects.

d, Occludin (green) was present in control (WT) but not in Occludin morphants. Nuclei are shown in blue.

Supplementary Table 2.1. Partial list of genes downregulated in *tcf2*^{2169} mutant larvae.

Figure 2.1 Gut lumen formation in WT and *tcf2*^{2169} mutant larvae

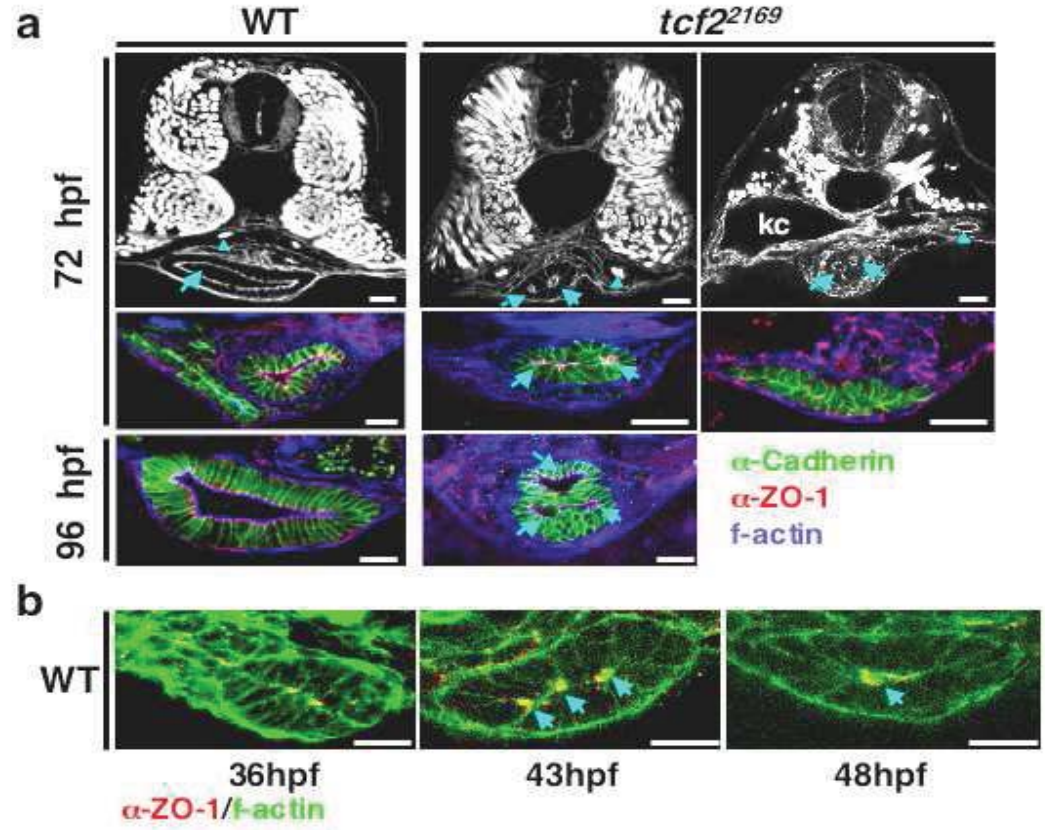

Bagnat et al. Figure 1

Figure 2.2 Tcf2 controls Cldn15 expression in the gut

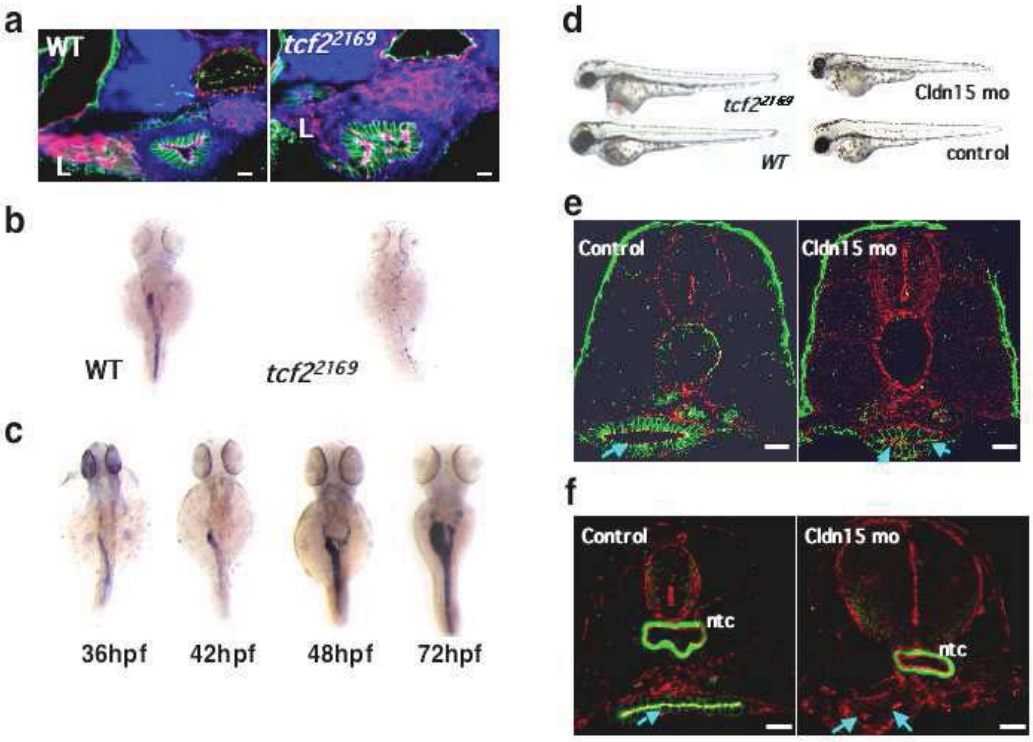

Bagnat et al. Figure 2

Figure 2.3 Cldn15 forms a paracellular ion pore

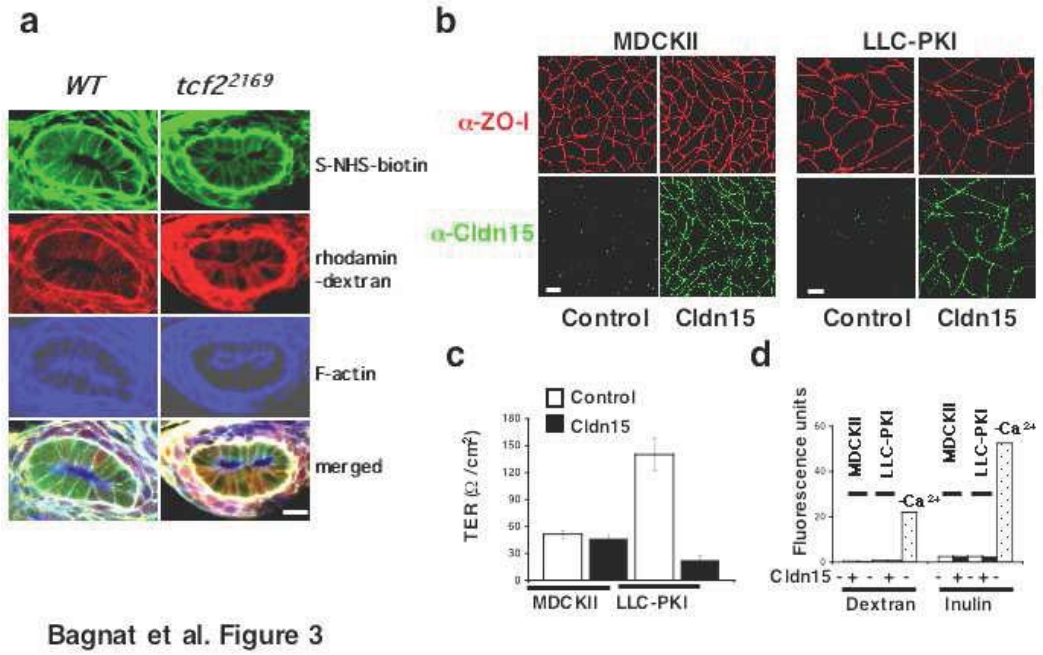

Bagnat et al. Figure 3

Figure 2.4 Cldn15 promotes single lumen formation through a fluid-driven mechanism

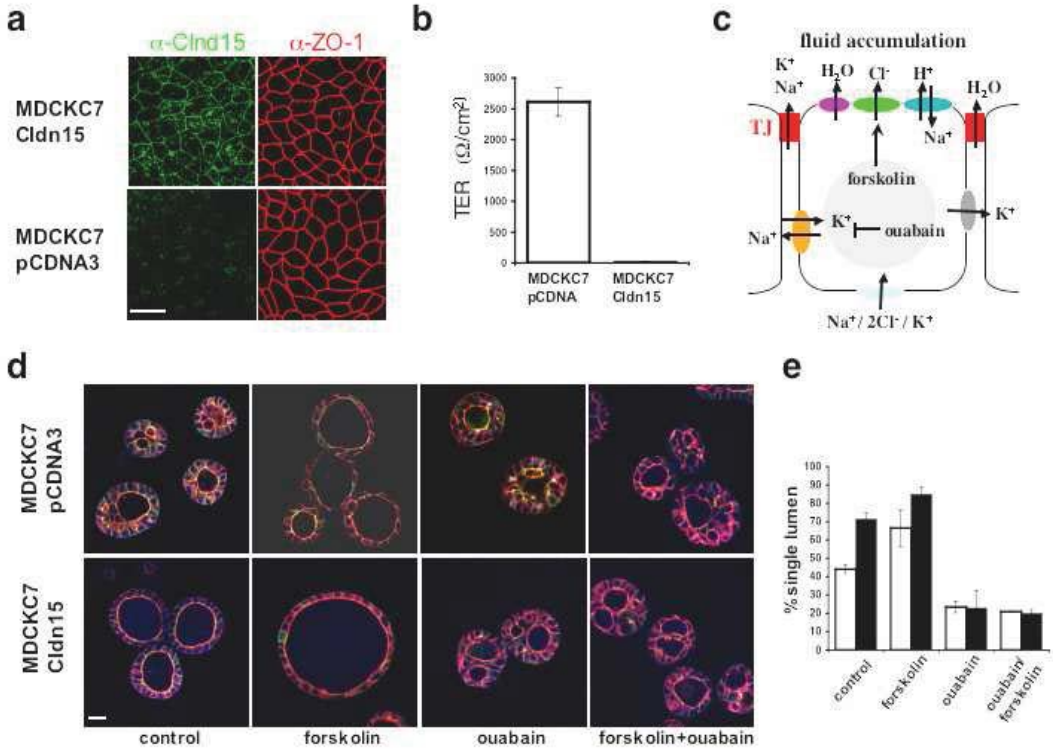

Bagnat et al. Figure 4

Figure 2.5 Disruption of the Na^+/K^+-ATPase-dependent electrochemical gradient blocks lumen coalescence

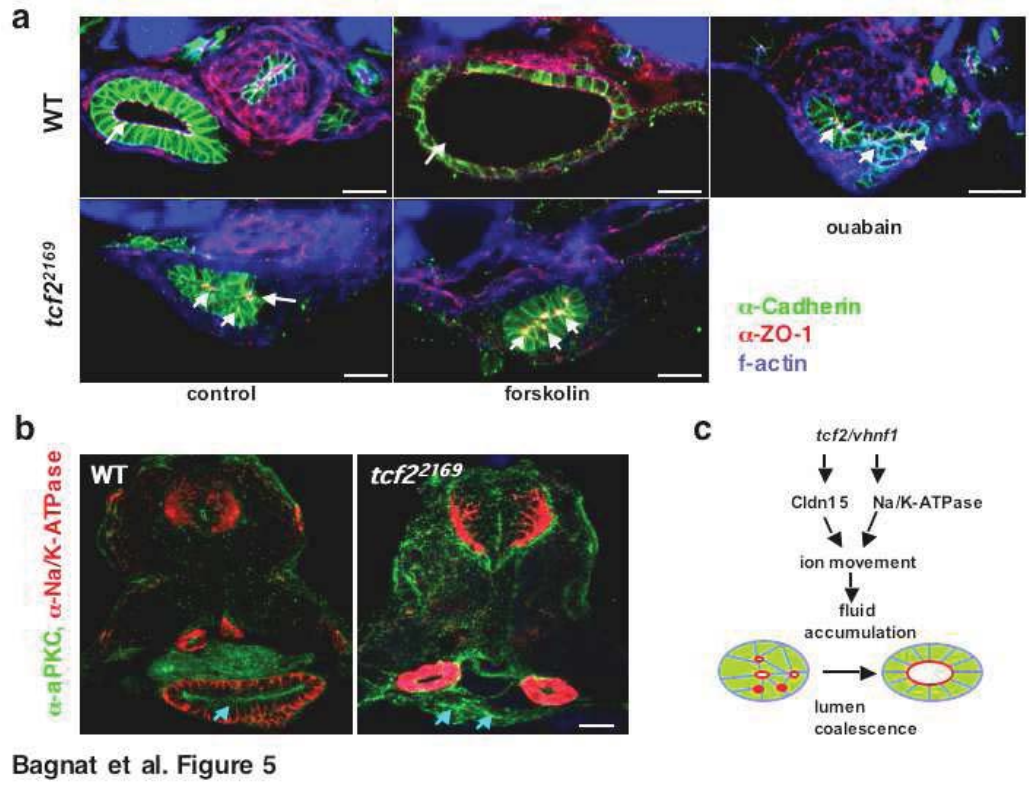

Bagnat et al. Figure 5

Supplementary Figure 2.1

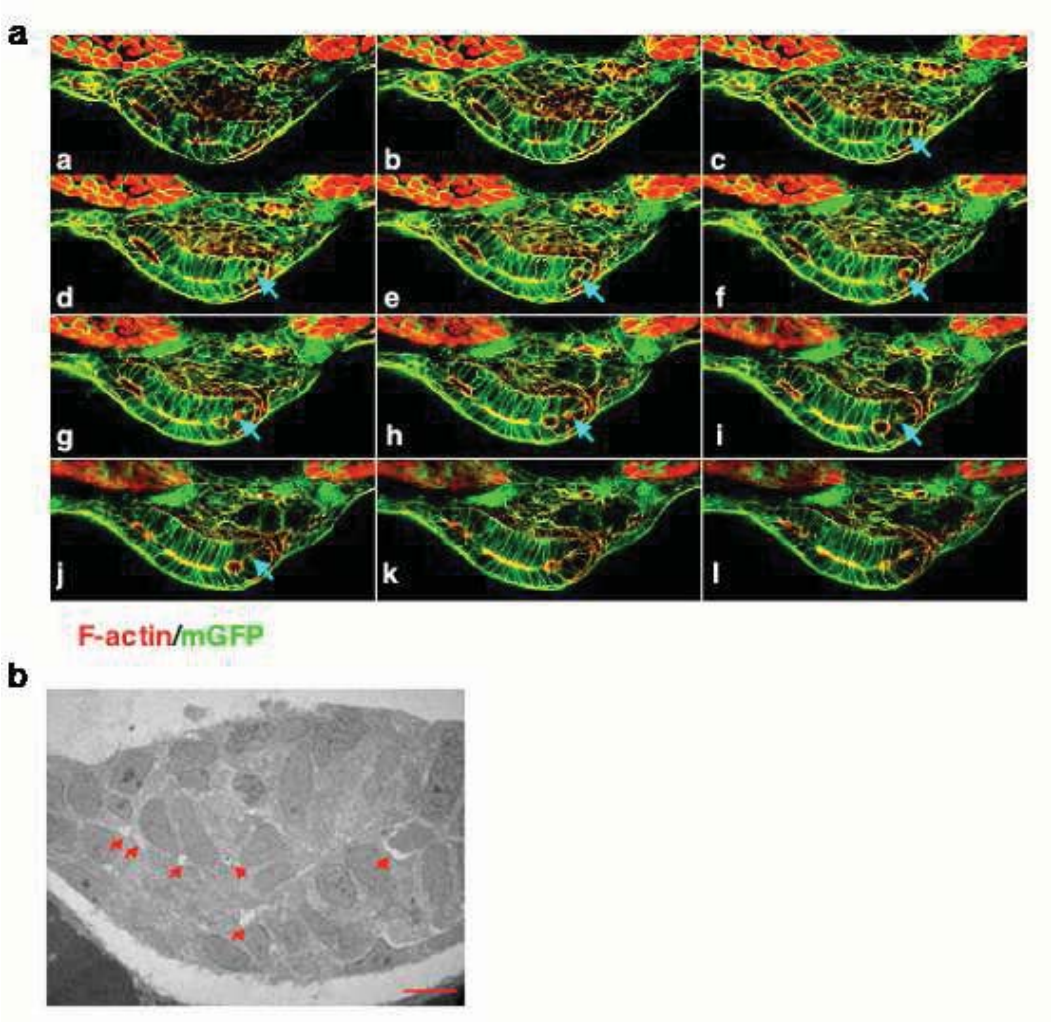

Bagnat el al. Supplementary Figure 1

Supplementary Figure 2.2 Apical membrane formation and gut lumen specification.

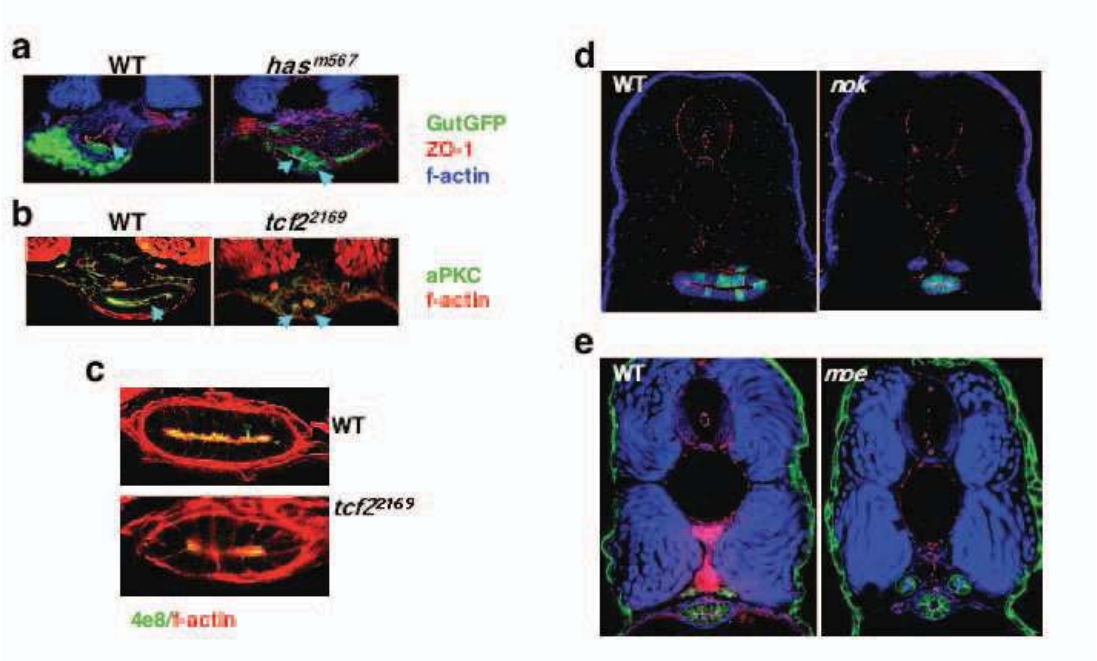

Bagnat el al. Supplementary Figure 2

Supplementary Figure 2.3

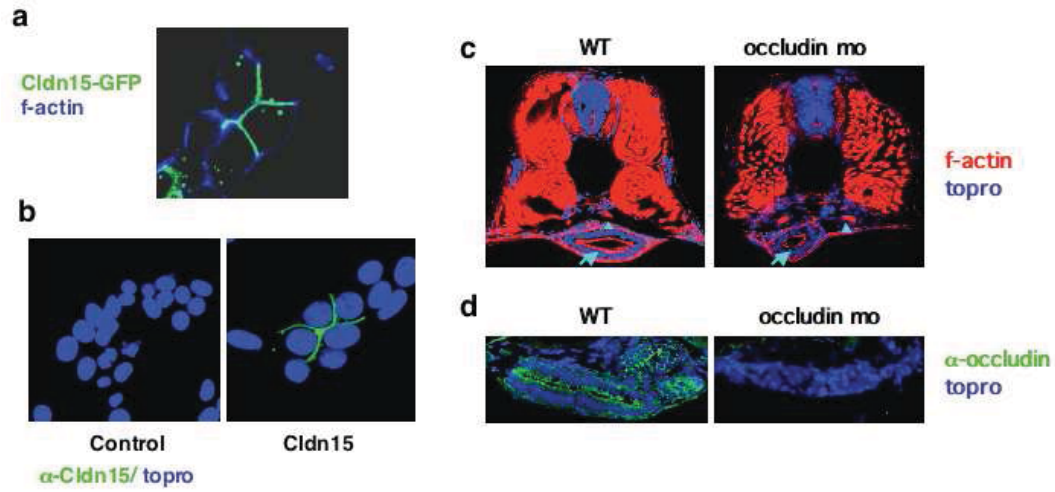

Bagnat el al. Supplementary Figure 3

Supplementary Table 2.1 Partial list of genes downregulated in *tcf2*^{2169} mutant larvae.

Gene	Accession number	Fold reduction
chymotrypsin B	BC076035	32.6
somatostatin	NM_131727	31.5
Gelsolin	Zgc:55779	28.6
carboxypeptidase A	NM_001002217	22.6
fatty acid binding protein, liver specific	NM_152960	20.1
trypsinogen	NM_199605	20
Apo-D	TC269968	16.7
trypsin	NM_131708	15.8
connexin 32.3	NM_199612	14.4
Zgc:103583	NM_001005598	12.9
USP21	BC003130	11.7
glucagon	NM_001008595	9.1
keratin alpha 2	TC291723	7.7
slc10a2	NM_200358	7.54
keratin gamma 3	TC267997	6.2
Slim3	TC275104	6.1
slc25a31	NM_200715	6
RNF38	TC273473	5.6
cldn15	NM_200404	5.3
AP-1 sigma	Zgc:56704	4.6
keratin 18	TC282646	4.1
atp1b2b	NM_131838	3.1
PDZ dom. containing 1 like	BC066762	2.5
Rho-GEF 10	CK680488	2.5

Bagnat el al. Supplementary Table 1

Chapter 3:

Regulation of intrahepatic ductal morphogenesis by Claudin-15likeb

Abstract

The intrahepatic biliary ducts in the liver serve an important function of transporting bile produced by hepatocytes to the digestive tract. Heritable diseases, such as Alagille Syndrome and polycystic liver disease (PLD) are caused by defects in biliary cell differentiation and biliary tract remodeling, respectively. While the signaling cascade involved in biliary cell differentiation has been extensively investigated, less is known about the cellular behavior underlying biliary duct remodeling. Here, we have identified a novel gene, *claudin-15likeb(cldn15lb),* which has an unique expression profile in hepatocytes and biliary epithelial cells. Claudins are junction proteins that have been implicated in the maintenance of epithelial polarity, regulation of paracellular transport, and providing barrier function. Zebrafish *cldn15lb* mutants exhibit defects in biliary ductal morphogenesis where biliary epithelial cells remain clustered together and form a disorganized network. Some hepatocytes do not appear to be properly polarized although junctions are formed. Preliminary results suggest that remodeling of the biliary ductal network is slower in the *cldn15lb* mutants. These data suggest that Cldn15lb may play a role in directing the remodeling process during biliary duct morphogenesis. c*ldn15lb* mutants provide the first *in vivo* model to study the role of tight junction proteins in the remodeling of the biliary ductal network.

Introduction

The liver is a vital organ with many essential functions, one of which is bile production for lipid metabolism. Hepatocytes are the primary cells in the liver that produces bile. The bile is then secreted to the digestive system where it functions to emulsify fats. The intrahepatic biliary ductal system is a network of tubes that permeates throughout the liver. These tubes carry bile away from the hepatocytes and collectively drain into the digestive system.

There are two tubular networks within the liver – the intrahepatic biliary ductal system and the vasculature. These two networks must be organized into a functional three-dimensional structure to ensure that bile and various hormones produced by the hepatocytes are transported to its proper location efficiently. Rows of hepatocytes form a polarized epithelium where the basolateral and apical surfaces are lined by the sinusoidal endothelial cells of the vasculature and the biliary epithelial cells (BECs) of the ductal network, respectively. Situated in hepatocytes between these two surfaces are tight junctions. They circumscribe the apex of hepatocytes to form a canaliculus through which bile is secreted and collected into the biliary ductal network. These tight junctions serve two functions – they create a blood-biliary barrier by regulating paracellular passage of small molecules and ions and they serve as a physical scaffold to separate apical and basolateral domains to maintain hepatic polarity.[1] Claudins are one of the core components of tight junctions. *In vitro* studies using WIF-B9 cells showed that claudin-2 is required for canalicular formation and maintenance of hepatic polarity.[2] Tight junctions are also found in BECs that form the biliary ductal network.[1] Expression profiles of claudins in intrahepatic ducts have been characterized and have

been proposed to be useful markers of biliary tract cancer diagnosis and prognosis.[3] Furthermore, mutations in tight junction proteins Claudin-1 and ZO-2 are responsible for certain intrahepatic cholestasis diseases.[4]

Epithelial morphogenesis is the driving force in creating and maintaining the architecture of the liver, yet the underlying molecular mechanism is less understood. In addition to being important for hepatocyte differentiation, the transcription factor HNF4a has been shown to orchestrate liver morphogenesis by regulating polarization.[5] Hepatocytes of *hnf4a* mutant mice do not form normal cell-cell contacts and expression of various cell junction proteins, including those of tight junctions, are downregulated.[5, 6] The resulting liver has small lesions and has lost its cohesive architecture.[5] Detailed analysis of hepatic polarity in zebrafish revealed that it coincides with development of the vascular and biliary ductal network, suggesting that polarization of hepatocytes is linked to the patterning of the two tubular networks. [7]

Several signaling pathways have been identified to be involved in BEC proliferation and differentiation but much less is known about the cellular behaviors that give rise to the intrahepatic biliary ductal network. In mammals, bile ducts are formed via sequential radial differentiation where the initial bilayer ductal plate is composed of one layer of differentiated BECs and one layer of hepatoblasts. Driven by Notch and TFGβ signaling, the second layer of hepatoblast differentiates to BECs to form a mature duct.[8, 9]

However, the development of the intrahepatic ductal network in teleost utilizes a different mechanism.[10, 11] Lorent et al reported that a notch-responsive fluorescent transgenic reporter zebrafish, Tg(Tp1bglob:eGFP), labels differentiated BECs and thus

was used to characterize the morphogenetic process.[12, 13] BECs undergo massive proliferation but it is unclear whether BEC differentiation is involved.[13] Live imaging of cultured zebrafish liver revealed that the founder population of BECs undergoes extensive and dynamic remodeling to generate a functional ductal system.[13] The authors observed filopodia continuously extending and retracting from these cells to sense and connect with their neighbors and cell bodies of BECs constantly rearranging to remodel the network.[13] However, molecules that mediate the dynamic remodeling process are unknown. In addition, whether similar remodeling occurs in mammals is unknown.

In this study, we identified a novel gene in the claudin family of tight junction proteins, claudin-15likeb(cldn15lb), that has a unique expression pattern in the liver and showed that it plays a role in the formation of the intrahepatic ductal network.

Results and Discussion

Identification of a novel alternatively spliced claudin gene.

From our microarray analysis in the previous study[14], we identified a novel transcript (NM_001002446) that encodes a protein belonging to the large PMP22/EMP/MP20/claudin superfamily. This protein contains 4 transmembrane domains, 2 extracellular loops, and a PDZ-binding domain characteristic of the topology of the claudin family of proteins. The first extracellular loop also contains the signature WGLWCC motif present in all claudins. These evidences suggest that this transcript encodes a claudin protein. Alignment with other claudin proteins identified this novel transcript to be phylogenetically related to mammalian Claudin-15 (Fig 3.1a), which also shares significant homology to mammalian Claudin-10[15]. The transcript was subsequently named *claudin-15likeb (cldn15lb)*.

Genomic structure analysis identified this transcript to be encoded in five exons. Further investigation of the EST database revealed another five-exon transcript from the same gene that resulted from alternative splicing of the first exon(Fig 3.1b). The two transcripts, *cldn15lb_transcript variant1(cldn15lb_tv1)* and *cldn15lb_transcript variant2*(*cldn15lb_tv2)*, share the last four exons and only differ in the first exon. The first exon encodes the first transmembrane and first extracellular loop.(Fig 3.1b) The amino acid composition of the first extracellular loop determines the barrier properties of each claudin[16] and as such, the two variants are believed to convey different barrier properties and functions. Interestingly, mammalian Claudin-10 was previously described to be also alternative spliced in the first exon similar to *cldn15lb.*[17, 18] It has six transcript variants that are each differentially expressed in various tissues and exhibit

different functions[17]. Three of the six mammalian transcripts lack the fourth exon and these protein localizes with calreticulin and/or in vesicular structures suggesting that they may play a novel role within the cell.[17] Additional *cldn15lb* transcripts lacking exon 4 are not found in the zebrafish EST database.

In situ hybridization analysis was performed to study the expression pattern of the two transcripts. Transcript specific probes targeting the first exon of each transcript revealed that the two transcripts are expressed differentially. *cldn15lb_tv1* is not maternally deposited(Fig 3.2a). At 42hpf, its expression was detected in the liver and continues to be expressed at 72hpf (Fig 3.2a). In addition, minimal expression was observed in the gut and pancreas starting at 60 and 72hpf, respectively (Fig. 3.2a). Closer examination of the liver expression at 72hpf revealed that *cldn15lb_tv1* is expressed in a tree-like pattern (Fig. 3.2a') similar to that of the two tubular networks in the liver. However, the *cldn15lb_tv1* probe did not mark endothelial cells that expresses Tg(flk1:GFP) and its expression was still present in *cloche* mutants which lacked most endothelial cells(Fig. 3.2c). These data suggest that *cldn15lb_tv1* is not expressed in the vasculature. Instead, it is likely that *cldn15lb_tv1* is expressed in the biliary ductal network. In contrast, the second transcript, *cldn15lb_tv2*, is maternally deposited and expressed mainly in the head and gut starting at 42hpf (Fig. 3.2b). We also detected *cldn15lb_tv2* expression in the liver at 72hpf but it did not appear as a branched structure similar to the first transcript(Fig 3.2b). Taken together, the two transcript variants of the *cldn15lb* gene are expressed dynamically and in different tissues during zebrafish development.

To determine the cellular localization of Cldn15lb protein, a peptide antibody was generated. The first extracellular loop which determines barrier properties and the intracellular c-terminal region of the protein juxtaposed to the last transmembrane are the most variable regions of claudin proteins.[19] As such, a peptide sequence in the c-terminal region was chosen as a target for the antibody(Fig 3.2d). To validate the antibody, we transfected HEK293 cells that do not express endogenous claudins with a construct encoding either zebrafish Cldn10, Cldn10like, Cldn15lb-a or Cldn15lb-b. (Cldn15lb-a is protein encoded by *cldn15lb_tv1* and Cldn15lb-b is encoded by *cldn15lb_tv2*) The antibody did not label cells transfected with Cldn10 or Cldn10like but did label those transfected with either Cldn15lb transcripts(Fig. 3.2e). To validate that the antibody is recognizing Cldn15lb, I generated GFP-tagged version of the two isoforms and transfected them into Cos7 cells. Only cells transfected with either GFP-tagged constructs are labeled by the antibody. Non-transfected cells are not labeled(Fig 3.2f). These results suggest that the antibody recognizes Cldn15lb but does not distinguish between the two isoforms.

To determine cellular localization of Cldn15lb in the zebrafish, we performed immunocytochemistry using the antibody we generated. In 80hpf wildtype embryos (Fig. 3.2g), Cldn15lb co-localizes with the expression of notch-responsive fluorescent reporter gene (Tg(Tp1bglob:eGFP)) suggesting that Cldn15lb is expressed in BECs. The antibody also labeled the hepatocytes and gut epithelial cells at slightly lower levels. Since the antibody recognizes both isoforms of Cldn15lb, it is likely that it is detecting Cldn15lb-b in the gut in accordance with the *in situ hybridization* data. Cldn15lb expression becomes markedly enhanced in the BECs at 100hpf while its expression in the

hepatocytes becomes more punctated (Fig. 3.2h). At 120hpf, Cldn15lb is only expressed in the BECs (Fig. 3.2i). It must be noted that the antibody might be detecting both isoforms of Cldn15lb in the liver since both transcripts are expressed in the liver at 72hpf. In addition, the antibody also labeled the neuromasts of the lateral line (data not shown) which expresses other claudins such as Cldnb[20], suggesting that this antibody may cross-react with other members of the claudin family. In summary, Cldn15lb is initially expressed in both hepatocytes and BECs and its localization becomes restricted to biliary ductal network by 120hpf.

We have identified two isoforms of Cldn15lb that is expressed in a tissue- and cell-specific manner. It is possible that cldn15lb-a is an ortholog of human Cldn10 because it is also expressed in hepatocytes and BECs.[3, 14] However, mouse Cldn10 is only weakly expressed in tight junctions of hepatocytes as revealed by immunofluorescence microscopy.[18] Cldn15lb-b may be an ortholog of mammalian cldn15 as both are expressed in the gut. Whether both isoforms exhibit the same paracellular permeability functions as their respective orthologs remains to be investigated.

Cldn15lb is important for hepatocyte polarization and biliary development.

To determine the role of cldn15lb in the development of the biliary network in the zebrafish liver, we analyzed the cldn15lb^{fh290} mutant from the TILLING project at FHCRC.[21] The mutant contains the nonsense point mutation C290T located at the 3'-end of the exon1a, and thus, it is specific to *cldn15lb-tv1*(Fig. 3.3a). Its position corresponds to the end of the first extracellular loop, resulting in a truncated protein(Fig.

3.3a). Mutant larvae do not exhibit any body phenotype(Fig 3.3b). Furthermore, expression of *foxA3* and *Cp* is normal indicating that general endoderm and liver development, respectively, is not affected(data not shown). The mutants can survive to adulthood with no observable phenotype. Immunohistochemistry of 100hpf larvae with the Cldn15lb antibody did not show reactivity in the mutant liver suggesting that the full-length, functional Cldn15lb-a is absent in the mutants (Fig 3.3c). However, the antibody still recognizes Cldn15lb-b in the gut in both wildtype and mutant larvae. These data further support that the antibody is detecting Cldn15lb-a and not Cldn15lb-b in the liver. In addition, *cldn15lb_tv1* transcripts in the liver and pancreas are decreased in the mutant while *cldn15l_tv2* expression in the gut is not affected (Fig 3.3d).

Between 50hpf and 80hpf, hepatocytes receive signals from invading endothelial cells and undergo polarization.[7] The apical and basolateral domains of hepatocytes are defined and this dictates the location of the biliary ducts and vasculature, respectively.[7] Hepatic polarization is a crucial step in liver morphogenesis because it establishes the architecture of the two tubular networks. Since claudins are members of the tight junctions that have been suggested to be involved in the maintenance of the apico-basolateral polarity[22], we asked whether hepatocytes were properly polarized in the mutant at 80hpf. In the wildtype livers, most hepatocytes lining the primitive biliary ducts are columnar in shape indicating that these cells are fully polarized. However, there is a small population, usually on the periphery of the liver, that is cuboidal-shaped indicating these cells are not polarized. In contrary, most hepatocytes in mutant livers are cuboidal in shape and are often found in rosettes (Fig. 3.4a). The defect in hepatic polarization does not seem to be completely penetrant since a small number of columnar

cells can be found in mutants livers. This might be caused by partial rescue by other claudins due to redundancy in the genome, especially since Cldn15lb_b is expressed in the liver at 72hpf.

While the shape of the hepatocytes suggest that polarization is affected in the mutant, adherens junction protein aPKC is properly localized to the apical membrane of hepatocytes (data not shown). Furthermore, we also observed "kissing-point" contacts between membranes characteristic of tight junctions in electron micrographs of 4dpf and 5dpf mutant livers (Fig. 3.4b-c) suggesting that functional junctions are formed. Since adherens junction proteins are recruited to the apical junctional complex before claudins[22], it is not surprising that they are localized properly in the *cldn15lb* mutant. However, it is surprising to observe functional junctions in the mutant electron micrographs. It is possible that these junctions belong to the small population of fully polarized hepatocytes. Furthermore, these electron micrographs were of larvae at later stages where other claudins may have partially rescued the phenotype. Analysis of earlier stages was technically challenged.

In addition to its role in establishing the architecture of liver, setting up apico-basal polarity is necessary for directional cellular trafficking which delivers pumps and transporters to the proper domains where they can serve their function. Apical transporters and pumps such as BSEP and MDR1-6 are directed to the canalicular membrane where they act to secrete bile.[23] Knockdown of Rab11a, which is involved in apical targeting in polarized epithelial WIF-B9 cultured cells, disrupted canalicular formation.[24] Since polarization might have been affected in cldn15lb mutant, we asked whether trafficking is also affected and consequently disturbs canalicular formation.

Using an antibody against a canalicular transporter, we found canaliculi in wildtype larvae to be long indentations into the apical domain of hepatocytes. (Fig. 3.4d) However, in the mutants, the canaliculi appear to be shorter and wider suggesting that development of mutant canaliculi is stunted. (Fig. 3.4d) It appears that canalicular proteins are not properly trafficked to the apical membrane. Consistent with the hepatocyte polarity defects being not completely penetrant, two-thirds of the mutant larvae recover and exhibit normal canaliculi by 6dpf (data not shown). Since the canaliculi are not properly developed, we hypothesized that bile secretion, and thus lipid metabolism, is also disrupted. However, processing of quenched fluorescent lipid PED6 and fatty acid metabolism assay (Farber lab, personal communication) revealed that lipid metabolism is normal in the mutants (data not shown).

Next, we further characterized tight junctions formation in mutant hepatocytes. Preliminary immunohistochemistry analysis of tight junction protein Zona Occludens-1 (ZO-1) indicated that it is localized properly in the apical membrane but its expression level is decreased in the mutants. This phenotype is in agreement with a previous study in which loss of zebrafish Cldn5a in the neuroepithelium does not affect localization of ZO-1.[25] Furthermore, in liver-specific knockout of E-Cadherin in mouse, ZO-1 was localized properly and canaliculi development was normal suggesting that hepatic polarization is dispensable for development of the hepatic epithelium.[6] However, another study showed that decreased expression of tight junction, adherens junction, desmosomes, and gap junction proteins in Hnf4α mutant mice led to defects in liver architecture.[5]. Thus, the role of tight junctions in the formation of liver architecture remains unsolved. Additional analysis with other members of the zona occludens family

and membrane protein Occludin in the Cldn15lb mutants will be useful to determine if tight junctions are formed and maintained in the absence of Cldn15lb. These data may help in understanding why junctions are observed in electron microscopy. The observed junctions might be in the small population of fully polarized cells or it is possible that Cldn15lb, like E-cadherin, is not necessary for junction formation in hepatocytes.

Defects in biliary ductal network remodeling.

Given its specific expression in the biliary ductal network, we decided to investigate the role of cldn15lb in the development of biliary network. We found that at 100hpf, the ductal network in the mutants is disorganized. (Fig. 3.5a) There are ectopic connections between cell bodies of BECs in the mutants. Also, the cell bodies are in closer proximity to each other in the mutants.

Lorent et al have described that the biliary ductal network undergoes population expansion via proliferation between 80hpf and 100hpf and extensive remodeling between 3 and 4dpf to give rise to the highly elaborate network.[13] To determine whether it is a defect in proliferation control or remodeling that gave rise to a disorganized biliary ductal network in the mutants, we analyzed the structure of the network at various stages from 50hpf to 120hpf. Both wildtype and mutant embryos have similar numbers of BECs at all stages suggesting that cldn15lb does not play a role in proliferation of BECs (data not shown). We also characterized the architecture of the network and found that the network structures are comparable in the wildtype and mutant larvae at 74hpf (Fig. 3.5b) and 80hpf (Fig. 3.5c). These stages were described to have dynamic remodeling.[13] However, at 100hpf, we began to observe a difference in the placement of the cell bodies.

(Fig. 3.5d) In wildtype larvae, most cell bodies of the BECs have undergone remodeling and are separated from each other. They each exist as single entities and are only connected to each other by cytoplasmic bridges. Conversely, most of the cell bodies in the mutants are clustered together in groups of 4 or more. To quantify this phenotype, we counted the percentage of BECs that existed as single, double, triple, or 4 or more cells. There is a significant decrease in the percentage of BECs that were single cells and an increase in the percentage of BECs that were in clusters of 4 or more cells in the mutant larvae (Fig. 3.5e). The difference in double and triple cells between wildtype and mutant larvae is not statistically significant.

At 70hpf, BECs are clustered together as chains of cells.[13] During remodeling from 70hpf to 96hpf, BECs separate from each other so that they are only connected by cytoplasmic bridges which will become the future ducts.[13] BECs accomplish this by 1) progressive lengthening or shortening of cytoplasmic bridge between two adjacent BECs, 2) migration of a single BEC via a cytoplasmic extension, or 3) dynamic extension and retraction of filopodia to connect with its neighbor.[13] The cldn15lb mutant appears to be inefficient in this process such that cells never migrate away from each other and cytoplasmic bridges never form.

To further understand the inefficiency in remodeling, live imaging can be used to visualize the entire the remodeling process. Preliminary live imaging experiments reveal that BECs in the mutants do not send out as many protrusion and those that do form move at a slower pace. We were not able to capture migrating cell to determine if there are any defects in cytoplasmic bridge lengthening/shortening or cell body migration.

Additional imaging with optimized parameters is necessary to better visualize this process in real-time.

The identification of the novel *cldn15lb*^{fh290} mutant has provided a tool to study the role of tight junction proteins in biliary ductal network development. Cldn15lb has a dynamic expression profile in hepatocytes and BECs. In the absence of Cldn15lb, the biliary ductal network is disorganized due to defects in remodeling. While much is known about BEC differentiation, understanding the cellular behaviors that contribute to the formation of a functional three-dimensional network will also be important in understanding diseases caused by defects in remodeling of nascent tract.

Materials and Methods

Animals. AB wild-type and mutant allele *cldn15lb*^{fh290} were maintained as described previously.[26] The *cldn15lb*^{fh290} mutation was crossed into Tg(Tp1bglob:eGFP)[13] and genotyped according to the TILLING center protocol with XbaI[21].

***In situ hybridization*.** Whole-mount *in situ hybridizations* were performed as described previously.[27] The *cldn15lb_tv1*(accession number NM_001002446) and *cldn15lb_tv2* (Table 3.1) *in situ* probes correspond to the first exon of each transcript. The *in situ* constructs were cloned into pGEMT-easy (Promega) with *Bam* HI/*Xho* I. Antisense DIG-labeled RNA probes for both genes were made by linearizing the construct with *Xho*I and transcribed with T7 RNA polymerase. For *in situ hybridization* with immunohistochemistry, *in situ hybridization* experiment was performed first. The larvae were then sectioned with a vibratome and processed as described below (under immunohistochemistry).

Expression vectors and cell transfection. Both cldn15lb transcripts were amplified by PCR from RNA of wildtype larvae at 3dpf and cloned into mammalian expression vector pCDNA3 (Invitrogen) with BamHI/NotI. The eGFP construct was cloned into pCDNA3 by NotI/XhoI. HEK293 cells were cultured in DMEM/10%FBS and Cos7 cells were cultured in H21 High Glucose media/10%FBS/Pen-Strep to 95% confluency for transfection. Transient transfections were performed with Lipofectamine2000 (Promega) and Opti-MEM medium (Life Technologies). Transfected cells were fixed with 10% trichloroacetic acid, washed with PBS, and stained as previously described.[28]

Generation of peptide antibody. The program AnthePro 6.0 was used to analyze the protein sequence and to identify the peptide sequence. General Biosciences Corporation synthesized the peptide, conjugated it to KLH, and used it to immunized two rabbits (GB9 and GB10). We received antisera from the second and third bleeds. The Nab™ Protein A Plus Spin Kit(Pierce) was used for purification. The first eluted fraction was used for immunofluorescence and immunohistochemistry studies.

Immunohistochemistry. For staining with cldn15lb antibody serum, larvae were fixed in Histochoice™MB®(Electron Microscopy Sciences) at 4°C overnight. The fixed larvae were embedded in 4% low-melt agarose in PBS. Transverse sections 150µm or 200µm thick were obtained with a vibratome (Leica, Bannockburn, IL, USA). Sections were incubated with primary antibodies overnight at 4°C. Sections were then washed and incubated with Alexa Fluor conjugated secondary antibodies. After washing, sections were mounted on slides in Vectashield and imaged on a Zeiss LSM510 Pascal confocal microscope. Images were further analyzed with LSM software (Zeiss, Thornwood, NY, USA) and Image J Software. For whole-mount staining, larvae were fixed in 4% formaldehyde in egg water at 4°C overnight. The fixed larvae were washed in PBS. The skin and yolk was removed to expose the endoderm. The samples were incubated with antibodies and processed as above.

Transmission electron microscopy. The larvae were fixed with 0.8%paraformaldehyde/ 2.5% glutaraldehyde in 0.1M Cacaodylate buffer at 4°C overnight. The samples were processed and stained by the Pathology & Imaging Core of the Liver Center at the University of California, San Francisco.

References

1. Lee, N.P. and J.M. Luk, *Hepatic tight junctions: from viral entry to cancer metastasis.* World J Gastroenterol. **16**(3): p. 289-95.
2. Son, S., et al., *Knockdown of tight junction protein claudin-2 prevents bile canalicular formation in WIF-B9 cells.* Histochem Cell Biol, 2009. **131**(3): p. 411-24.
3. Nemeth, Z., et al., *Claudin-1, -2, -3, -4, -7, -8, and -10 protein expression in biliary tract cancers.* J Histochem Cytochem, 2009. **57**(2): p. 113-21.
4. Carlton, V.E., L. Pawlikowska, and L.N. Bull, *Molecular basis of intrahepatic cholestasis.* Ann Med, 2004. **36**(8): p. 606-17.
5. Parviz, F., et al., *Hepatocyte nuclear factor 4alpha controls the development of a hepatic epithelium and liver morphogenesis.* Nat Genet, 2003. **34**(3): p. 292-6.
6. Battle, M.A., et al., *Hepatocyte nuclear factor 4alpha orchestrates expression of cell adhesion proteins during the epithelial transformation of the developing liver.* Proc Natl Acad Sci U S A, 2006. **103**(22): p. 8419-24.
7. Sakaguchi, T.F., et al., *Endothelial signals modulate hepatocyte apicobasal polarization in zebrafish.* Curr Biol, 2008. **18**(20): p. 1565-71.
8. Antoniou, A., et al., *Intrahepatic bile ducts develop according to a new mode of tubulogenesis regulated by the transcription factor SOX9.* Gastroenterology, 2009. **136**(7): p. 2325-33.
9. Zong, Y., et al., *Notch signaling controls liver development by regulating biliary differentiation.* Development, 2009. **136**(10): p. 1727-39.

10. Hampton, J.A., et al., *Functional units in rainbow trout (Salmo gairdneri, Richardson) liver: II. The biliary system.* Anat Rec, 1988. **221**(2): p. 619-34.

11. Hardman, R.C., et al., *An in vivo look at vertebrate liver architecture: three-dimensional reconstructions from medaka (Oryzias latipes).* Anat Rec (Hoboken), 2007. **290**(7): p. 770-82.

12. Parsons, M.J., et al., *Notch-responsive cells initiate the secondary transition in larval zebrafish pancreas.* Mech Dev, 2009. **126**(10): p. 898-912.

13. Lorent, K., et al., *Reiterative use of the notch signal during zebrafish intrahepatic biliary development.* Dev Dyn. **239**(3): p. 855-64.

14. Bagnat, M., et al., *Genetic control of single lumen formation in the zebrafish gut.* Nat Cell Biol, 2007. **9**(8): p. 954-60.

15. Loh, Y.H., et al., *Extensive expansion of the claudin gene family in the teleost fish, Fugu rubripes.* Genome Res, 2004. **14**(7): p. 1248-57.

16. Van Itallie, C.M. and J.M. Anderson, *Claudins and epithelial paracellular transport.* Annu Rev Physiol, 2006. **68**: p. 403-29.

17. Gunzel, D., et al., *Claudin-10 exists in six alternatively spliced isoforms that exhibit distinct localization and function.* J Cell Sci, 2009. **122**(Pt 10): p. 1507-17.

18. Van Itallie, C.M., et al., *Two splice variants of claudin-10 in the kidney create paracellular pores with different ion selectivities.* Am J Physiol Renal Physiol, 2006. **291**(6): p. F1288-99.

19. Van Itallie, C.M. and J.M. Anderson, *The molecular physiology of tight junction pores.* Physiology (Bethesda), 2004. **19**: p. 331-8.

20. Haas, P. and D. Gilmour, *Chemokine signaling mediates self-organizing tissue migration in the zebrafish lateral line.* Dev Cell, 2006. **10**(5): p. 673-80.

21. *Fred Hutchinson Cancer Research Center(FHCRC) Zebrafish TILLING Project.* www.zfishtilling.org.

22. Shin, K., V.C. Fogg, and B. Margolis, *Tight junctions and cell polarity.* Annu Rev Cell Dev Biol, 2006. **22**: p. 207-35.

23. Alrefai, W.A. and R.K. Gill, *Bile acid transporters: structure, function, regulation and pathophysiological implications.* Pharm Res, 2007. **24**(10): p. 1803-23.

24. Wakabayashi, Y., et al., *Rab11a and myosin Vb are required for bile canalicular formation in WIF-B9 cells.* Proc Natl Acad Sci U S A, 2005. **102**(42): p. 15087-92.

25. Zhang, J., et al., *Establishment of a neuroepithelial barrier by Claudin5a is essential for zebrafish brain ventricular lumen expansion.* Proc Natl Acad Sci U S A. **107**(4): p. 1425-30.

26. Jensen, A.M. and M. Westerfield, *Zebrafish mosaic eyes is a novel FERM protein required for retinal lamination and retinal pigmented epithelial tight junction formation.* Curr Biol, 2004. **14**(8): p. 711-7.

27. Alexander, J., D.Y. Stainier, and D. Yelon, *Screening mosaic F1 females for mutations affecting zebrafish heart induction and patterning.* Dev Genet, 1998. **22**(3): p. 288-99.

28. Horne-Badovinac, S., et al., *Positional cloning of heart and soul reveals multiple roles for PKC lambda in zebrafish organogenesis.* Curr Biol, 2001. **11**(19): p. 1492-502.

Figure Legends

Fig. 3.1 Identification of a novel alternatively spliced claudin gene.

a, Phylogenetic tree of mammalian and zebrafish Claudin-10 and Claudin-15 proteins show that the novel protein, highlighted in yellow, is most similar to mammalian Claudin15. This tree was constructed with neighbor joining and 1000 bootstrap replicates. Zebrafish(dr), Human(hs), Mouse(mm), rat(rn).

b, Schematic of the claudin-15like1b gene. This is a 5 exon gene and the first exons, 1a and 1b, are alternatively spliced to generate 2 transcripts. The first exon encodes the first transmembrane and first extracellular loop. Purple boxes represent the coding regions for each transmembrane domain in the protein. Purple lines represent the part of the transcript recognized by the transcript variant-specific *in situ hybridization* probes.

Fig. 3.2 Expression pattern of cldn15lb in zebrafish.

In situ hybridization with transcript variant-specific probes.

a, *cldn15lb_tv1* is not expressed at the 2-cell stage. At 42hpf, it is expressed mainly in the liver(arrow) with some minor expression in the head. Its expression in the liver intensifies through 60hpf and 72hpf. Minor expression is observed in the pancreas at 72hpf(arrowhead)

a', Detailed analysis at 72hpf shows that expression in the liver is in a unique, tree-like pattern.

b, *cldn15lb_tv2* is detected at 2-cell stage indicating that it is maternally deposited. *cldn15lb_tv2* transcripts can be found in the gut(arrow) and head at 42hpf. Minimal expression of *cldn15lb_tv2* is found in the liver at 72hpf(arrowhead).

c, left, *in situ hybridization* of *cldn15lb* in wildtype and *cloche* mutant larvae which lacks endothelial cells. Probe used was against the 3'UTR of *cldn15lb* so it labels both transcripts. Right, cross section of *in situ hybridization* with fluorescent microscopy. *In situ hybridization* signal does not co-localize with GFP-positive endothelial cells. *cldn15lb* does not seem to be expressed in endothelial cells of the vasculature.

d, Sequence alignment between zebrafish Cldn10, Cldn15, Cldn15lb-a, Cldn15lb-b, and Cldn10l. Purple box indicates transmembrane regions. Red box highlights the epitope targeted by the peptide antibody we generated.

e, HEK293 cells were transiently transfected with constructs expressing Cldn10l, Cldn15, Cldn15lb-a, and Cldn15lb-b. Immunofluorescence with peptide antibody generated against Cldn15lb recognized Cldn15lb only.

f, Cos7 cells were transiently transfected with untagged or GFP-tagged version of either transcript variant. The antibody serum recognized cells that were transfected with either untagged transcript and it co-localized with the GFP-tagged version. The polyclonal antibody in the serum reacts to Cldn15lb but does not distinguish between the 2 isoforms.

g-i, Transverse sections of 150um through the liver at 80hpf **(g)**, 100hpf **(h)**, and 120hpf **(i)**. Green: Tg(Tp1bglob:eGFP), red: antibody serum. At 80hpf, Cldn15lb is expressed in the biliary epithelial cells (BECs) (arrows) and the surrounding hepatocytes. Its expression in BECs (arrows) increases while that in the hepatocytes becomes more punctated at 100hpf. At 120hpf, Cldn15lb is only expressed in BECs (arrows). The antibody also recognizes Cldn15lb-b in the gut(g).

Fig 3.3 Characterization of cldn15lb TILLING mutant

a, Schematic of the TILLING mutation. The nonsense mutation is situated at the end of exon1a making this mutation specific to *cldn15lb_tv1*. The mutation is situated immediately before the second transmembrane region.

b, Brightfield picture of the wildtype and mutant larvae at 5dpf. The overall body morphology is normal.

c, Transverse sections of 150um through the liver at 100hpf. Green: Tg(Tp1bglob:eGFP), red: antibody serum. Wildtype larvae (top) express Cldn15lb in BECs (arrows). Expression in mutant larvae (bottom) is markedly decreased (arrow) or absent (arrowhead).

d, *in situ hybridization* analysis at 80hpf with a probe that recognizes both transcript variant. In addition to having a smaller liver and pancreas, the expression level of *cldn15lb_tv1* is decreased in these organs.

Fig 3.4 Hepatic polarization and bile canaliculi development are affected in cldn15lb mutant larvae

a, Whole-mount analysis of 80hpf embryos stained for pan-cadherin (green) and ZO-1 (red). Pan-cadherin marks hepatocytes and BECs with higher intensities. ZO-1 outlines the vasculature. Hepatocytes that neighbors BECs(*) are columnar in the wildtype larvae and cuboidal in mutant larvae. More hepatocytes are found in rosette patterns (●) in mutant larvae than in wildtype larvae.

b-c, Electron microscopy at 4dpf**(b)** and 5dpf**(c)**. Junctional complexes can be found in both wildtype and mutant larvae.

d, Whole-mount analysis of 100hpf Tg(lfabp:rasGFP) larvae stained for SPGP (red) which marks canaliculi. Canaliculi in mutant livers are not as fully developed as those in wildtype livers.

Fig 3.5 Defects in biliary ductal network remodeling in cldn15lb mutant larvae

a, Whole-mount confocal projections of Tg(Tp1bglob:eGFP) at 100hpf. Biliary ductal network in the mutant livers are disorganized with ectopic ducts.

b-c, Whole-mount confocal projections. Time-course analysis of Tg(Tp1bglob:eGFP) during the remodeling of the ductal network. The number of cells and structure of the network appear normal at 74hpf and 80hpf.

d, At 100hpf, a majority of the BECs exists as single entities in wildtype livers. In the mutant livers, multiple BECs are clustered together at this stage(boxed regions). Blue=TOPRO

e, Percentage of BECs that exists as single cells, doubles, triples, or clusters of 4 or more. Wildtype livers have almost double the number of single cells and almost 3 times less cells in 4 or more cells clusters. (* $p = 0.00056$, ** $p = 0.006$)

Figure 3.1 Identification of a novel alternatively spliced claudin gene

a

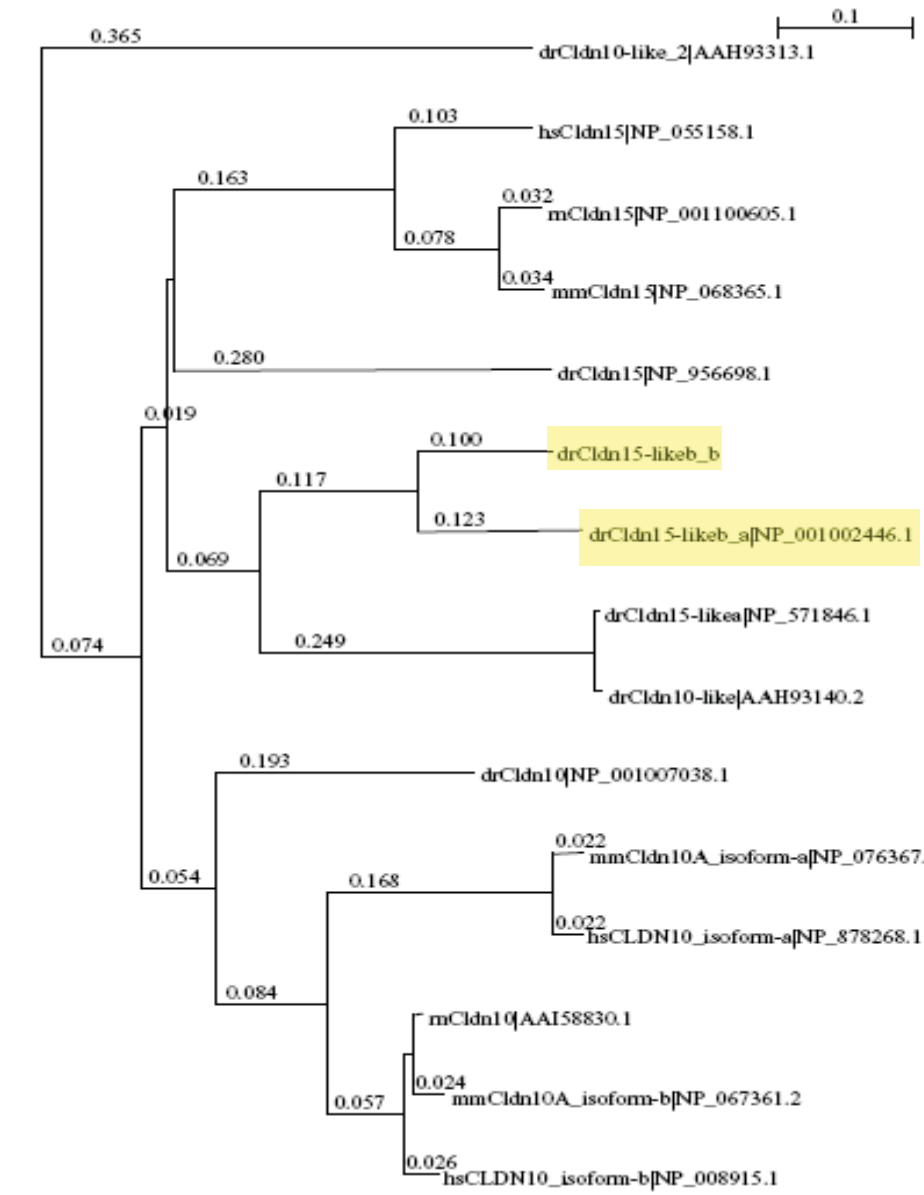

b

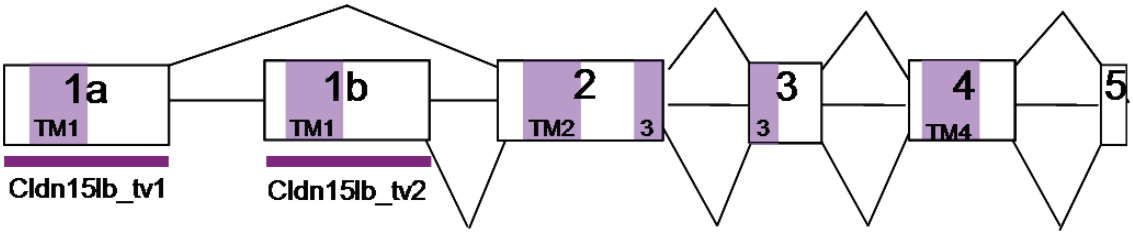

Figure 3.2 Expression pattern of *cldn15lb* in zebrafish

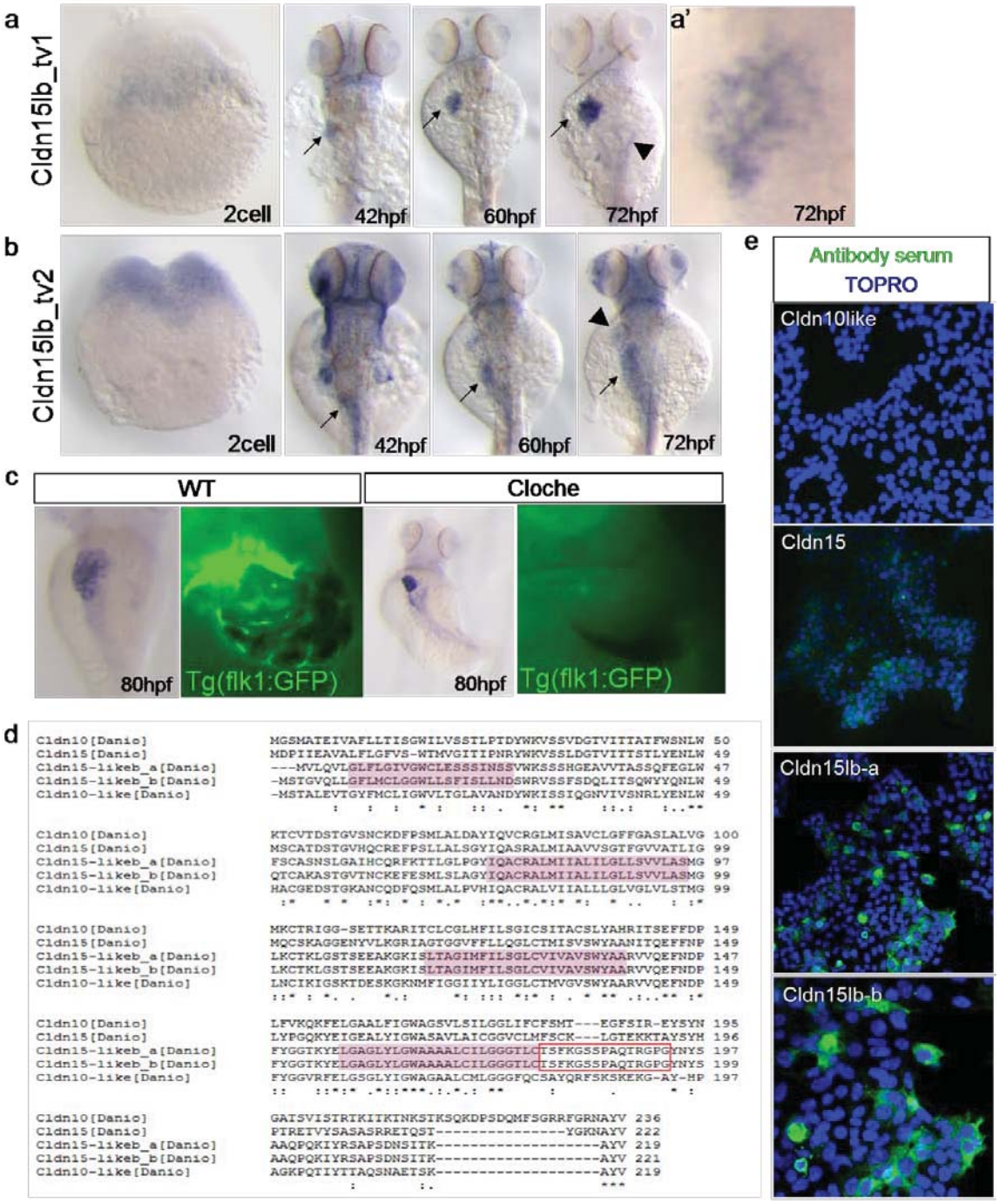

Figure 3.2 Expression pattern of cldn15lb in zebrafish – continued

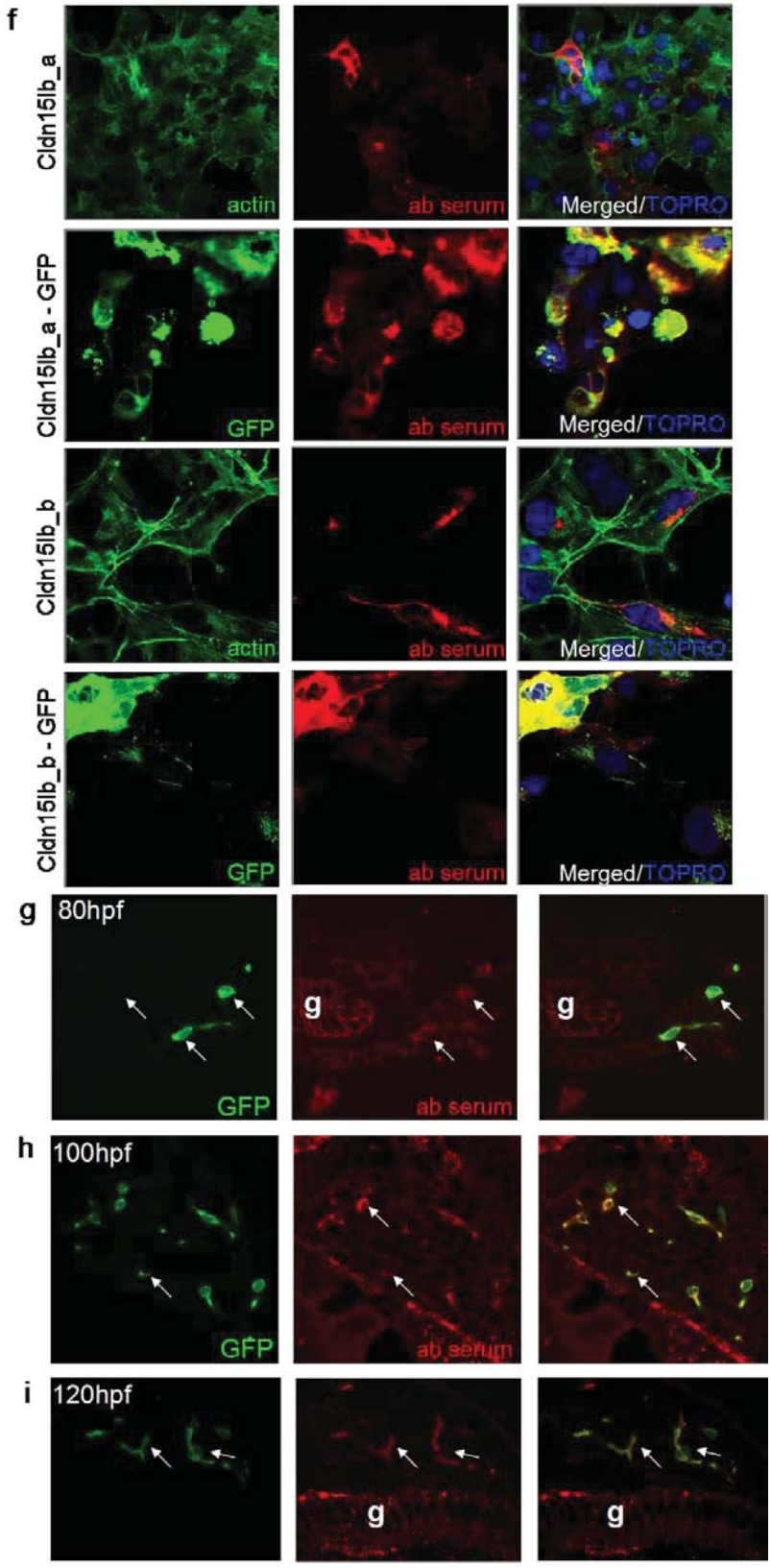

Figure 3.3 Characterization of *cldn15lb* TILLING mutant

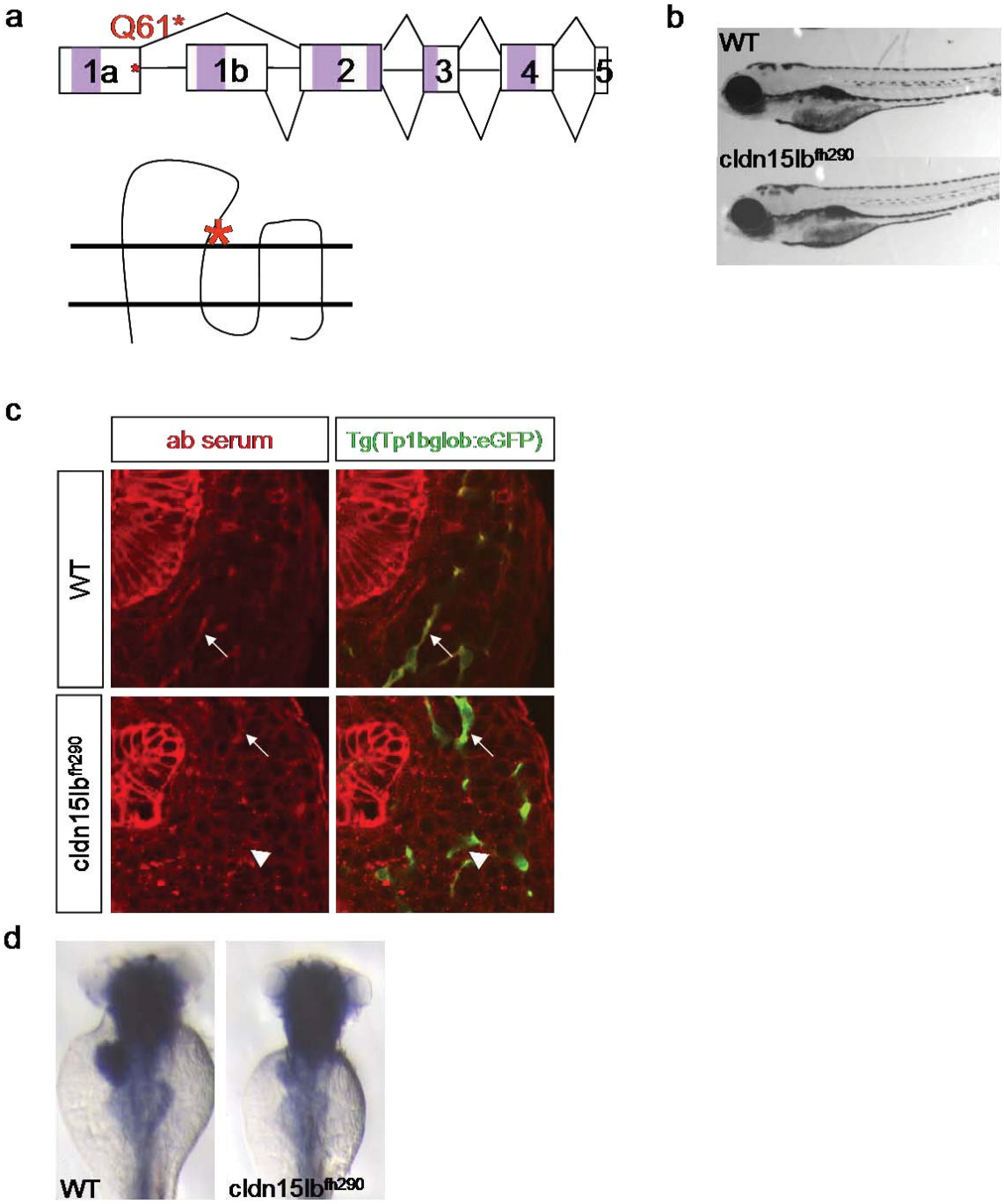

Figure 3.4 Hepatic polarization and bile canaliculi development are affected in *cldn15lb* mutant larvae

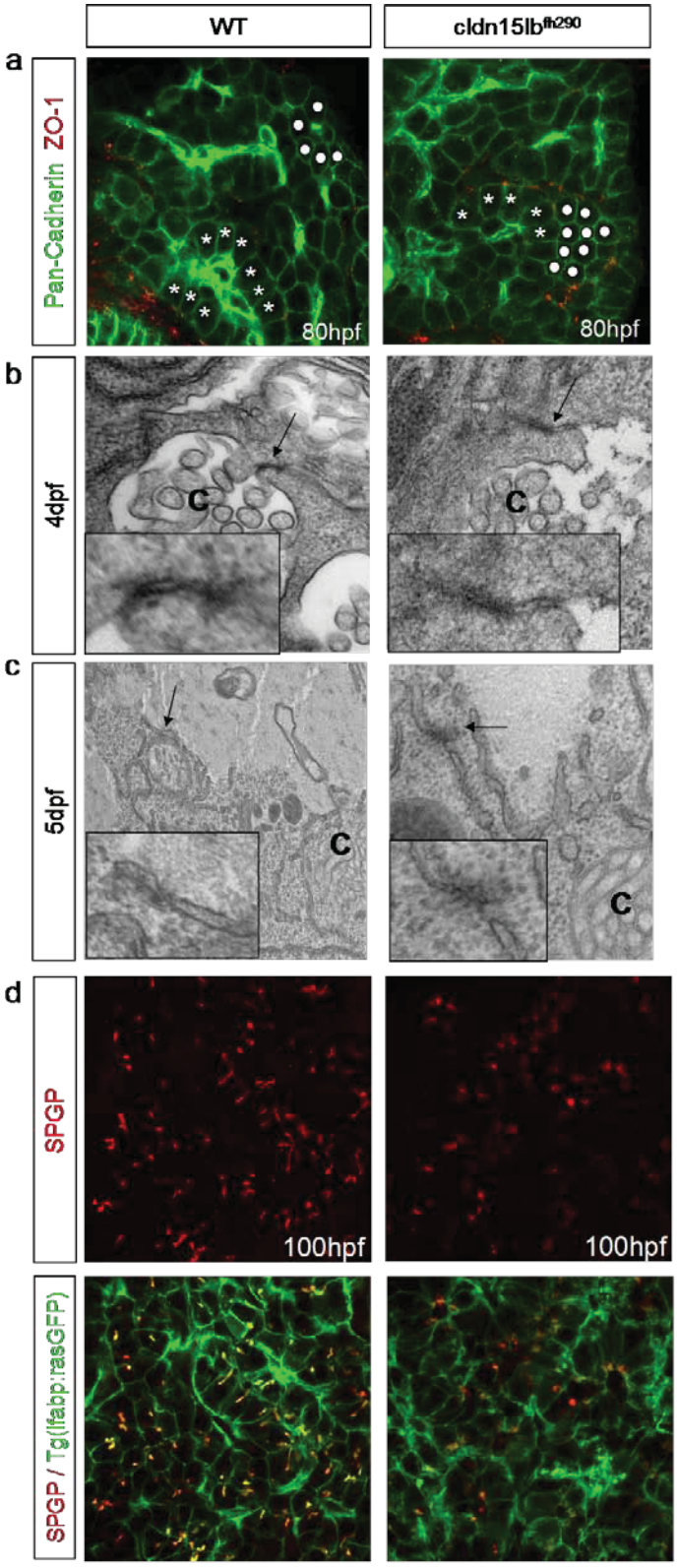

Figure 3.5 Defects in biliary ductal network remodeling in *cldn15lb* mutant larvae

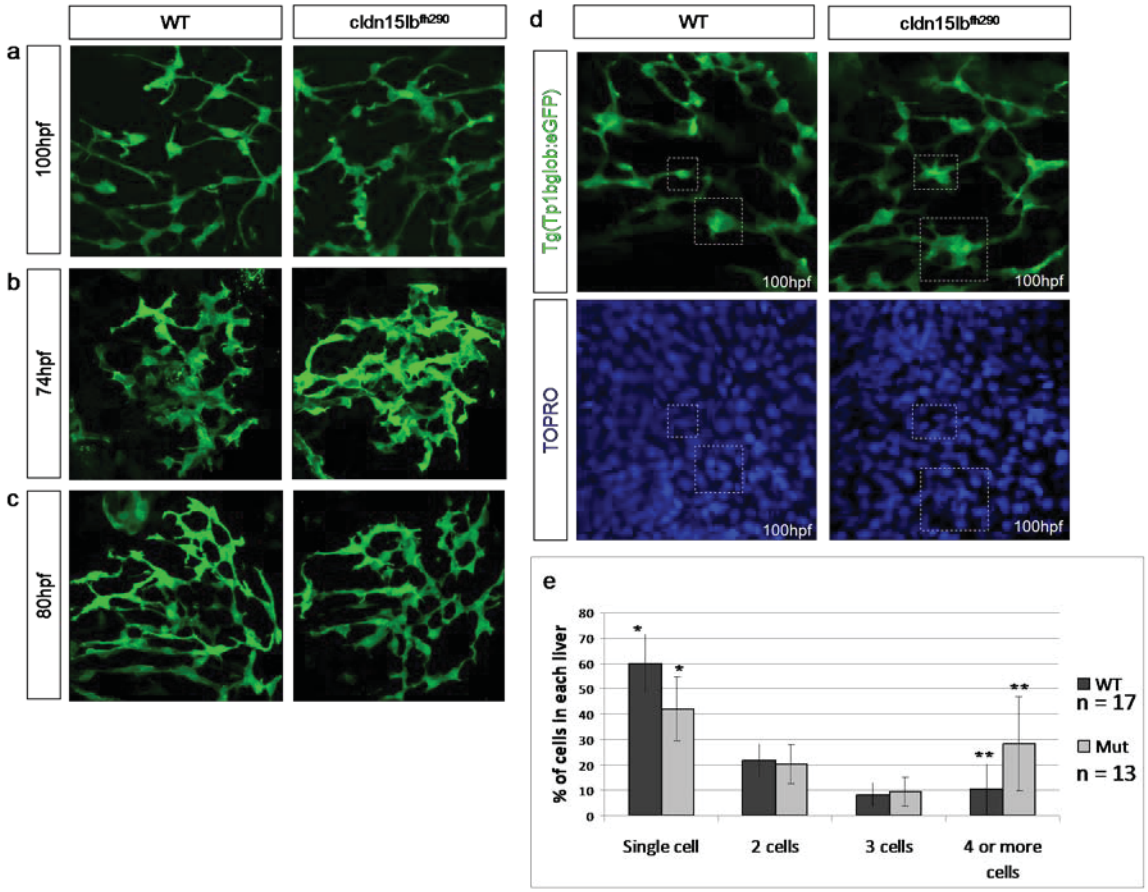

Table 3.1 Sequence of *cldn15lb_tv2*

Exon	Sequence
1	ATGTCGACTGGTGTTCAGCTGCTGGGATTTTTGATGTGTTTGGGC GGCTGGCTGCTGTCCTTCATATCGCTGTTGAATGATTCGTGGCGA GTGTCCTCGTTTAGTGATCAGTTGATCACGTCTCAGTGGTATTAC CAGAATCTGTGGCAGACGTGTGCAAAGGCCAGCACCGGCGTCAC CAACTGCAAGGAGTTCGAGTCCATGCTCTCTCTGGCAG
2	GATATATCCAGGCTTGTCGGGCTCTGATGATCATCGCTCTGATTC TGGGTCTGCTGTCTGTGGTTCTGGCCTCGATGGGACTCAAGTGCA CTAAACTGGGCAGCACGTCTGAGGAGGCCAAGGGCAAAATCAGC CTGACTGCAGGAATCATTTCATCCTGTCAG
3	GTTTGTGTGTTATCGTGGCCGTGTCGTGGTACGCTGCTCGAGTCG TCCAGGAATTTAATGACCCGTTTTATGGAGGCACAAA
4	GTATGAACTGGGCGCGGGTCTGTATCTGGGATGGGCGGCAGCTG CTCTGTGTATATTAGGAGGAGGAACTCTCTGCACTTCCTTTAAAG GTTCATCTCCTGCACAAACACG
5	GGGCCCGGGCTACAACTACAGCGCTGCACAGCCTCAGAAGATTT ACAGATCTGCTCCATCAGACAACAGCATCACCAAAGCATATGTT TAA

Chapter 4:

Discussion

In this dissertation, I have reported our studies of zebrafish gut and biliary duct morphogenesis. We found that the homeobox gene *tcf2* genetically controls single lumen formation in the gut tube. It transcriptionally regulates the expression of *cldn15* and *Na^+/K^+-ATPase* and they in turn establish the electrochemical gradient necessary to drive fluid accumulation into the gut lumen. This fluid accumulation drives single lumen formation. In biliary duct morphogenesis, we found that *cldn15lb* expressed in the hepatocytes and biliary epithelial cells(BECs) mediates the remodeling of the nascent biliary ductal network. In the absence of Cldn15lb, remodeling is defective and the architecture of the biliary ductal network is not structured, although its function in lipid metabolism is not affected.

Role of Claudins in polarization

Claudins are the core proteins in tight junctions. Expression of Claudin-1 and Claudin-2 in L-fibroblasts which lack tight junctions is sufficient to induce cell aggregation and cell-cell contacts. These contacts form functional junctions based on observations of tight junction strands in freeze-fracture electron microscopy.[1] Tight junctions have been shown in various studies to be important for the establishment and maintenance of apico-basal polarity. (reviewed in [2]) Thus, it is reasonable to hypothesize that claudins are important for polarization. However, in both *cldn15* morphants and *cldn15lb* mutants, polarization does not seem to be fully disrupted. *Heart*

and soul, the *aPKCλ* (also known as *prkci*) mutant, has a polarization defect which resulted in a multiple lumen phenotype.[3] While *cldn15* morphants exhibit multiple lumen phenotype, we only observed mislocalization of the tight junction marker ZO-1 in less than half of the mutant larvae. Similarly, cell shape suggests that hepatocytes are not polarized in the *cldn15lb* mutants but junction proteins are properly localized and junctions are observed. The polarization defect appears to be only partially penetrant in claudin mutants. These data suggest that claudins are dispensable for polarization. This might be due to the fact that claudins are only recruited to the junction complex at the late stages of polarization after most polarity proteins have been deposited to the appropriate domains.[2] While claudins may not be essential for establishing polarity, it may be important for the maintenance of polarity. They act as a physical scaffold to reinforce the separation of the apical and basolateral domains which may be important for development or function of the epithelium.

Multiple cellular processes utilized in morphogenesis to create the appropriate microenvironment

A variety of cellular processes are required for morphogenesis. The combination of different processes utilized can produce a diversity of structures that provide different functions. While processes such as proliferation, apoptosis, and differentiation are important for establishing the correct number and type of cells for morphogenesis, processes such as cell rearrangement and polarization place the cells in the correct location and in the appropriate cellular state essential for epithelial morphogenesis.

In addition to these processes, I propose that the establishment of a proper microenvironment by tight junctions is also important for epithelial morphogenesis. Proper microenvironments include having suitable electrochemical gradient or pH levels.[4] In zebrafish brain ventricle development, Cldn5a works together with Na^+/K^+ ATPase to form the suitable electrochemical gradient necessary for ventricular lumen expansion. [5] Cldn15 deficient mice exhibit a megaintestine phenotype due to increased proliferation.[6] One hypothesis is that Cldn15 regulates the transport of certain growth factors and that inappropriate amounts of such factors in the microenvironment leads to increase in proliferation.[6] Non-ionic solutes that can permeate through tight junctions have not been identified but tight junctions are estimated to be permeable to solutes with diameters up to 4Å.[7, 8] Thus, it is possible that claudin-containing tight junctions can also regulate growth factors. Tight junctions can also create microenvironments within the apical and basolateral domains. In human airway epithelial cells, the growth factor ligand and its receptor are expressed in the same cell but segregated from each other by tight junctions.[9] After mechanical injury where the tight junctions are disrupted and the ligand and its receptor are no longer separated, growth factor signaling becomes activated.[9] Taken together, regulation of ionic and nonionic solute permeability by tight junctions creates the appropriate microenvironment necessary for normal morphogenesis.

In gut development, we have shown *in vitro* and *in vivo* that disruption of the electrochemical gradient by drugs or in *tcf2* mutants leads to multiple lumen formation. Here, I propose two models by which Cldn15lb may mediate biliary network remodeling. (Fig. 4.1) During the remodeling process, BECs must send out filopodia to sense their

neighbors. Meanwhile, there is a population of hepatocytes that lies between these BECs and their targets. Thus, intercellular spaces between hepatocytes must be made to allow these projections to grow. Cldn15lb that is expressed in hepatocytes at 80hpf form tight junctions in the row of hepatic epithelium. In one model, Cldn15lb-based tight junctions are regulating the paracellular transport of ionic solutes such that an electrochemical gradient is formed between rows of hepatic epithelium. This gradient can drive fluid accumulation to the region between the rows of hepatocytes and thus generate space. Cellular projections from BECs can now efficiently navigate to their targets along these "tracks". (Fig. 4.1a) In *cldn15lb* mutant larvae, a proper microenvironment is not established and thus, a "track" is not formed. Protrusions from mutant BECs have a difficult time navigating their way through the hepatocytes due to space constraints and thus are slower. (Fig. 4.1b) In the second model, Cldn15lb-based tight junctions are maintaining microenvironments within the apical and basolateral domains. In wildtype larvae, growth factors or guidance molecules (or their respective receptors) may be expressed in the apical domain of the hepatocytes. The filopodia express their molecular counterparts and thus, are guided along the apical domain to their targets. (Fig. 4.1a) In *cldn15lb* mutant larvae where growth factors or guidance molecules are not restricted to the apical domain, their effective concentration is lower. Without the proper guidance, the filopodia move slower in the mutant larvae. (Fig. 4.1b)

In vitro studies to characterize Cldn15lb permeability selectivity will help determine whether Cldn15lb can drive fluid accumulation as predicted in the first model. Higher resolution live imaging of the remodeling process will also be useful. We are currently generating transgenic fluorescent reporters (Tg(Tp1bglob:ras-mCherry)) to

label the cell membrane of BECs. Together with the Tg(lfabp:rasGFP) line which labels the cell membrane of hepatocytes (Appendix 2), we will be able to better characterize the remodeling process. To assay the second model, we need to find guidance cues that might be expressed in the liver and then perform loss-of-function analysis. It would be exciting if any molecules identified to be expressed in the liver are localized in a domain specific fashion in wildtype and mislocalized in the mutant larvae.

In summary, we have characterized the cellular processes involved in gut and biliary duct morphogenesis. It is important to have the proper microenvironment for the epithelium to undergo any morphogenetic process. It appears that in both the zebrafish gut and liver, claudins play a role in establishing this microenvironment and in the absence of claudins, epithelial morphogenesis is disrupted.

References

1. Furuse, M., et al., *A single gene product, claudin-1 or -2, reconstitutes tight junction strands and recruits occludin in fibroblasts.* J Cell Biol, 1998. **143**(2): p. 391-401.
2. Ng, A.N., et al., *Formation of the digestive system in zebrafish: III. Intestinal epithelium morphogenesis.* Dev Biol, 2005. **286**(1): p. 114-35.
3. Horne-Badovinac, S., et al., *Positional cloning of heart and soul reveals multiple roles for PKC lambda in zebrafish organogenesis.* Curr Biol, 2001. **11**(19): p. 1492-502.
4. Tsukita, S., et al., *Tight junction-based epithelial microenvironment and cell proliferation.* Oncogene, 2008. **27**(55): p. 6930-8.
5. Zhang, J., et al., *Establishment of a neuroepithelial barrier by Claudin5a is essential for zebrafish brain ventricular lumen expansion.* Proc Natl Acad Sci U S A. **107**(4): p. 1425-30.
6. Tamura, A., et al., *Megaintestine in claudin-15-deficient mice.* Gastroenterology, 2008. **134**(2): p. 523-34.
7. Van Itallie, C.M., et al., *The density of small tight junction pores varies among cell types and is increased by expression of claudin-2.* J Cell Sci, 2008. **121**(Pt 3): p. 298-305.
8. Watson, C.J., M. Rowland, and G. Warhurst, *Functional modeling of tight junctions in intestinal cell monolayers using polyethylene glycol oligomers.* Am J Physiol Cell Physiol, 2001. **281**(2): p. C388-97.

9. Vermeer, P.D., et al., *Segregation of receptor and ligand regulates activation of epithelial growth factor receptor.* Nature, 2003. **422**(6929): p. 322-6.

Figure Legend

Fig. 4.1. Proposed model of biliary duct morphogenesis

a, (Left) In wildtype, hepatocytes are fully polarized. Tight junctions and bile canaliculi are properly formed. **(Middle)** Cldn15lb-based tight junctions regulate paracellular transport to create the proper microenvironment for biliary duct morphogenesis. The appropriate microenvironment may be an electrochemical gradient that drives fluid accumulation to create space(yellow) for filopodia to travel through. It can also be an apical domain containing growth factors/guidance molecules(purple arcs) that directs filopodia extensions. **(Right)** With the appropriate microenvironment, filopodia extending from one biliary epithelial cell can navigate to their targets to form a functional network of ducts.

b, (Left) In cldn15lb mutants, hepatocytes may not be polarized and thus, are not columnar in shape. Formation of tight junctions may be incomplete and thus, are not fully functional. In addition, bile canaliculi development is stunted. **(Middle and right)** Without the fully functional tight junctions, the appropriate microenvironment cannot be established. Since no space is formed, the filopodia becomes physically constrained(⃠). It is also possible that growth factors/guidance molecules are distributed among the entire membrane and thus, its effective concentration is reduced. The filopodia does not receive the proper signal or level of signal and thus are not guided to its target.

Figure 4.1 Proposed model of biliary ductal morphogenesis

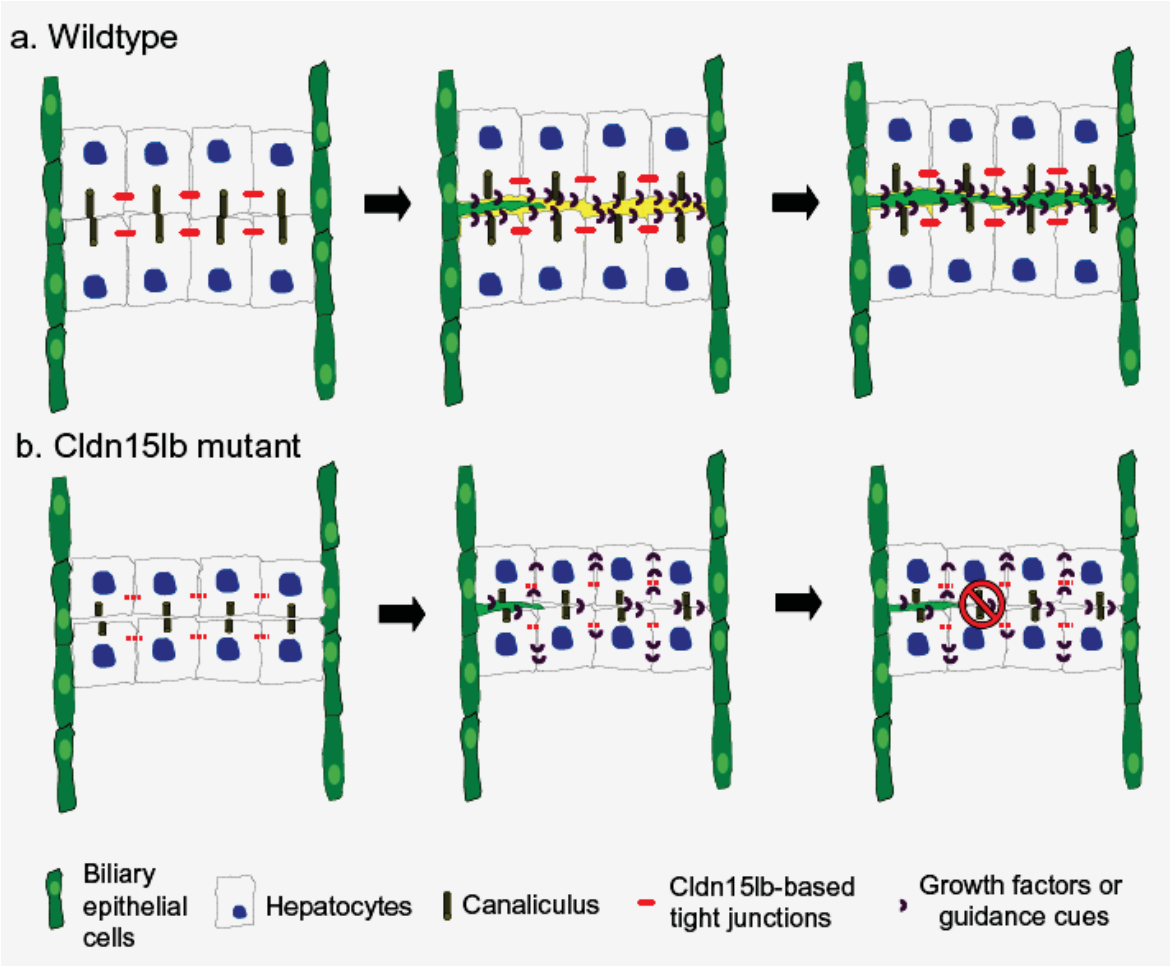

Appendix 1:

Understanding cell rearrangement and lumen expansion during gut tube formation

Introduction

Tubular organs of different size and function are formed using different mechanisms.[1] The zebrafish gut tube provides a great *in vivo* model to study the cord hollowing mechanism. In this mechanism, a population of epithelial cells undergoes polarization and a central lumen is formed at the apical membrane of these cells.[1, 2] In the zebrafish gut, the population of cells is initially in a disorganized state. During development, they rearrange themselves into a radial pattern and converge at a single, central point. This is the site of actin foci clustering and the site of the future lumen.[3] Polarization is thought to be involved in this process as mutation in the polarity protein aPKCλ (also known as Prkci) causes a defect in rearrangement resulting in a multiple lumen phenotype.[3] Furthermore, polarization defines the apical and basolateral domains. This definition is important for determining the site of lumen formation. The two domains are separated and maintained by the apical junction complex composing of adherens and tight junctions. Proper polarization is essential for regulated processes such as gas and nutrient exchange. However, how polarization and rearrangement are linked is unknown.

During cell rearrangement, cells exchange neighbors which require breaking and making new cell-cell contacts. This process requires dynamic cell adhesion where cell-cell interaction provided by adherens junctions is constantly modified. Cadherins, core

component of these adherens junctions, are molecules that form calcium-dependent cell-cell contacts with neighboring cells. They are transmembrane glycoproteins consisting of an extracellular domain that forms homophilic interaction and a cytoplasmic domain that interacts with the cytoskeleton. Establishment of cell-cell contacts has been demonstrated to coordinate cellular rearrangement and to play the role of an extracellular cell-surface organizer by recruiting other junction proteins to form the apical junction complex.[4, 5] Given the diverse roles of cadherin, it is likely that cadherin is a key molecular player for cell rearrangement and junction formation in zebrafish gut tubulogenesis.

After the cells have rearranged, a lumen must be generated to form a functional organ. Both the initial lumen formation and the subsequent lumen expansion require apical membrane biogenesis. During biogenesis, intracellular vesicles containing apical membrane components dock and fuse at the region of cell-cell contact.[6] These components give rise to an apical surface which continues to grow to delineate a lumen between the two layers of cells. Studies have also shown that adherens junctions act as the ‘targeting patch’ for such vesicle delivery.[7] Thus, defects in polarization or targeted delivery of polarized membrane components may disrupt lumen formation and growth in gut development.

Results

Our lab has shown that *prkci* and *claudin15* are important for single lumen formation while *mpp5a(nagie oko, nok)*, *epp4115(mosaic eyes, moe)*, and *occludin* are dispensible.[3, 8] To identify additional players important for cell rearrangement and the resulting single lumen formation, I analyzed lumen formation in Epithelial-cadherin (E-cadherin), Neural-cadherin (N-cadherin), and Crumbs2 mutants. There are several alleles of E-cadherin mutants with varying degree of phenotypes. ava^{tm94} is an allele with a mutation of a highly conserved amino acid in the extracellular domain. Based on the morphological phenotype, this allele is believed to have a dominant negative effect but this has not been proven.[9] ava^{tm94} mutants arrest in epiboly but zygotic-maternal dominant(ZMD) embryos, those that are heterozygous for the mutant locus in both the zygotic and maternal genomes, complete epiboly.[9] At 56hpf when a single lumen has formed in wildtype embryos, ava^{tm94} ZMD embryos exhibit a multiple lumen phenotype. (Fig. A1.1a) Surprisingly, this phenotype recovers by 72hpf and a single lumen is observed in the ZMD larvae. (Fig. A1.1b) The N-cadherin mutant, glo^{m117}, also has a defect in foci clustering which results in a multiple lumen phenotype. (Fig. A1.1c) Crumbs2 (*oko meduzy, ome*) is part of the apical junction complex involved in driving polarization and promoting formation and growth of the apical domain. Foci clustering in the Crumbs2 mutant, ome^{m98}, appears normal but the lumen is smaller than that of wildtype siblings. (Fig. A1.1d) Thus, it appears that in addition to Prkci and Claudin15, cadherins seems to play a crucial role in cell rearrangement.

To further characterize the role of cadherins during cell rearrangement and foci clustering, I analyzed the expression pattern of cadherins at different stages of gut

development in wildtype larvae with a pan-cadherin marker. I also used the tight junction marker ZO-1 to better understand tight junction formation during this process. At 36hpf (Fig. A1.2a), ZO-1 is localized to the apical side of gut epithelial cells at points of cell-cell contact, co-localizing with actin. Multiple cells appear to converge to a limited number of ZO-1 positive punctas. Cadherin is expressed on the lateral membrane with diffuse cytoplasmic expression in some cells. At 42hpf (Fig. A1.2b), cadherin localization is more focused on the lateral membrane. A few cells still have diffuse cadherin expression in the cytoplasm. Although there are more ZO-1 positive punctas at this stage, they are not present at every cell-cell contact. By 48hpf (Fig. A1.2c), cells have resolved to a radial pattern and most of the cells are columnar in shape. Cadherin is expressed as sharp boundaries in the lateral membrane and cytoplasmic cadherin is not observed. Furthermore, small lumens lined by f-actin are also observed. Additional ZO-1 positive tight junctions are present and they are present at every cell-cell contact. By 56hpf (Fig. A1.2d), cadherin is mainly on the subapical region. Lower amounts of cadherin are also observed at the basal region of the lateral membrane. ZO-1 labels the apex of each epithelial cell along the site of the future lumen. In summary, cadherin localization is very dynamic and ZO-1 positive tight junctions are continually formed as the gut undergoes morphogenesis.

In my effort study gut morphogenesis, I also analyzed an interesting mutant (FG7.3) from an ENU-induced mutagenic forward genetic screen.[10] These mutant larvae are less developed compared with their wildtype siblings. They have a smaller head and liver and exhibit cardiac edema starting at 4dpf. (Fig. A1.3a) Transverse sections through the gut reveal that the gut epithelium is thinner and the lumen is not

inflated. (Fig. A1.3b) Furthermore, expression of f-actin is decreased in the mutant larvae. (Fig. A1.3b) Most interestingly, we found that some apical and basal proteins are mislocalized in the mutant gut. 4B7, an antibody against an unknown antigen, labels the apical surface in wildtype larvae. In the mutant larvae, it labels both apical and basal domains. (Fig. A1.3c) Similarly, the basal marker 2H9 also labels both apical and basal domains in the mutant larvae. In addition, lateral surfaces of some cells are marked. (Fig. A1.3d) However, not all polarized proteins are affected. The apical antigen, 4E8, is properly localized in the mutant larvae. (Fig. A1.3e) In summary, the mutant FG7.3 appears to be less developed and displays an interesting phenotype whereby some, but not all, polarity proteins are mislocalized.

Discussion and Future Directions

Cadherin is a key molecule for cell rearrangement during gut morphogenesis

The expression profile of cadherin in the gut tube undergoes significant transformation during development. In the early stages of gut morphogenesis (Fig. A1.4a), cadherin is found on cell-cell membranes in a broad expression pattern and in a more punctated fashion around the perimeter of the gut. In addition, cadherin is found in the cytoplasm. ZO-1 is expressed at some, but not all, vertices of cell-cell contact. Presence of ZO-1 at some cell-cell vertices and the observation that more than two cells converge on each vertex suggest that some cells are polarizing and have initiated apical junction complex formation. Cells that do not express ZO-1 have not formed the apical junction complex. By 48hpf (Fig A1.4b), expression of cadherin is more defined in the lateral membrane and is no longer present on the basal surface. The basal surface is labeled by f-actin. Multiple small lumens have formed at the apical region of the epithelial cells. These lumens are defined by f-actin and circumscribed by ZO-1 which is present at every cell-cell contact. At this stage, the shape of each epithelial cell is columnar-like. The cell shape and presence of ZO-1 suggest that the epithelial cells are polarized. At 56hpf (Fig. A1.4c), cadherin expression becomes restricted to the subapical region of the lateral membrane. A lumen has formed in the apical domain which is devoid of cadherin but lined by f-actin and ZO-1 positive tight junctions. The epithelial cells are fully polarized and apical junction complexes are formed between every cell.

The dynamic expression pattern of cadherin molecules during cell rearrangement suggests that cell rearrangement and polarization are intimately linked. During cell rearrangement, adhesion between cells must be broken. Cell culture studies have shown

that endocytic trafficking of cadherins can mediate dynamic adhesion between cells. [11, 12] Furthermore, accumulating evidences have shown that cell-surface E-cadherin is actively endocytosed and recycled or degraded.[13, 14] The observed cytoplasmic cadherin at early stages of gut development could be such endocytosed vesicles. Subsequently, the cadherin molecules could be degraded which would explain the lack of cytoplasmic cadherins at 48hpf. Alternatively, the cadherin molecules can be recycled to the subapical region where ZO-1 –containing apical junction complex are being formed. Co-localization studies of E-cadherin with markers of trafficking organelles will determine if cadherin is being endocytosed and recycled or degraded during gut morphogenesis. Markers of early endosomes (Rab5, EEA1) and common endosomes (Rab4, Rab11) can be used to detect for endocytosis. Exocyst markers (Sec6, Sec8) can detect for exocytosis to the plasma membrane and lysosome markers (Rab7, LAMP-1) can identify E-cadherin that is targeted for degradation. Targeting expression of cadherins to the apical junction complex is one of the major steps in acquiring polarity. [15] This phenomenon is observed between 48hpf and 56hpf when cadherin expression becomes restricted to the subapical region and polarizing cells are acquiring columnar characteristics. In addition, delivery of cadherin molecules to the membrane allows adhesion to form between new neighboring cells after cell rearrangement. In all, this analysis highlights how regulation of adhesion, specifically of E- and N-cadherins, mediates and links epithelial cell rearrangement with polarization during gut morphogenesis. (Fig. A1.4)

It is important to note that cadherin is also found at the basal region of the lateral membrane at 56hpf. Since a pan-cadherin antibody against mouse antigen was used, the

antibody can be also labeling desmosomal cadherins which are usually found basal to the apical junction complex. It is also possible that E-cadherin has a yet unknown function in the basal region during gut development.

Given the important role of cadherin in cell rearrangement, it is not surprising that both E-cadherin and N-cadherin mutants have defects in single lumen formation. However, it was surprising that the E-cadherin mutant recovers and forms a single lumen at 72hpf. This might be because ZMD larvae were analyzed. The single copy of the wildtype allele may have rescued the phenotype. The exact function of the *ava*^{tm94} allele has not been investigated. The nature of the mutation may affect its function in gut morphogenesis in a novel way. Analysis of other mutant alleles of E-cadherin may provide additional insights into its role in cell rearrangement. However, attempts to analyze the *rk3* allele proved difficult as *rk3* homozygous mutant embryos exhibit variable phenotypes dependent on the parents and the temperature at which they are raised. (data not shown) The percentage of embryos exhibiting the weaker phenotype increases if the embryos are raised at 34ºC instead of the normal 28ºC.[16] Furthermore, there may be compensation by other cadherin genes such as N-cadherin in the zebrafish genome. Also, it would be interesting to investigate whether the *n-cadherin* mutant larvae also recover but unfortunately, they do not survive to 72hpf due to severe defects in the brain and body axis.

Apical membrane biogenesis drives lumen expansion and growth

Similar to the other apical membrane biogenesis mutants (*nok, moe*), mutation in *ome* also does not disrupt single lumen formation but instead, prevents lumen growth.

This phenotype might be due to the lack of apical membrane biogenesis. Intracellular vesicles containing apical membrane components dock and fuse at the region of cell-cell contact to generate additional apical membrane.[6] Targeted delivery of these vesicles to the apical membrane is essential for apical membrane biogenesis. FG7.3 mutant larvae appear to have a defect in targeted delivery since several polarized proteins are mislocalized. This defect can explain the smaller lumen phenotype observed in the mutant larvae. Interestingly, some proteins, such as those recognized by apical marker 4E8, are not affected. This data suggests that it may not be a general trafficking protein that is mutated in FG7.3. Identification of this gene will provide valuable insights into understanding directional protein trafficking and the role it plays in lumen expansion during gut morphogenesis.

It is also interesting to understand the role of Crumbs family of protein in polarization. Apical-basal polarity is disrupted and apical determinants are mislocalized in the retinal epithelium of *ome* mutants. [17] However, disruption of other Crumbs homolog in the pronephric duct and otic vesicle has no effect on polarity. [17] Furthermore, tight junction marker ZO-1 is apically localized in *nok* and *moe* mutants [8] suggesting that apico-basal polarity in the gut is also unaffected in these apical membrane biogenesis mutants. Thus, analyzing the localization of apical proteins in *ome* mutant guts will determine whether *crb2* is important for polarization in the gut.

Materials and Methods

Animals. AB wild-type, mutant alleles ava^{tm94}, *glo*^{m117}, *ome*^{m98}, and *Tg(gutGFP)*^{s854} were maintained as described previously.[18] FG7.3 was identified in a large-scale mutagenesis screen.[10]

Immunohistochemistry. Larvae were fixed in 4% formaldehyde in egg water at 4°C overnight. The fixed larvae were washed in PBS and embedded in 4% low-melt agarose in PBS. Transverse sections 200μm thick were obtained with a vibratome (Leica, Bannockburn, IL, USA). Sections were incubated with primary antibodies overnight at 4°C. Sections were then washed and incubated with Alexa Fluor conjugated secondary antibodies or Alexa Fluor conjugated phalloidin. After washing, sections were mounted on slides in Vectashield and imaged on a Zeiss LSM510 Pascal confocal microscope. Images were further analyzed with LSM software (Zeiss, Thornwood, NY, USA) and Image J Software.

References

1. Lubarsky, B. and M.A. Krasnow, *Tube morphogenesis: making and shaping biological tubes.* Cell, 2003. **112**(1): p. 19-28.
2. Pollack, A.L., R.B. Runyan, and K.E. Mostov, *Morphogenetic mechanisms of epithelial tubulogenesis: MDCK cell polarity is transiently rearranged without loss of cell-cell contact during scatter factor/hepatocyte growth factor-induced tubulogenesis.* Dev Biol, 1998. **204**(1): p. 64-79.
3. Horne-Badovinac, S., et al., *Positional cloning of heart and soul reveals multiple roles for PKC lambda in zebrafish organogenesis.* Curr Biol, 2001. **11**(19): p. 1492-502.
4. Gumbiner, B.M., *Regulation of cadherin-mediated adhesion in morphogenesis.* Nat Rev Mol Cell Biol, 2005. **6**(8): p. 622-34.
5. Le Bivic, A., *E-cadherin-mediated adhesion is not the founding event of epithelial cell polarity in Drosophila.* Trends Cell Biol, 2005. **15**(5): p. 237-40.
6. Vega-Salas, D.E., P.J. Salas, and E. Rodriguez-Boulan, *Exocytosis of vacuolar apical compartment (VAC): a cell-cell contact controlled mechanism for the establishment of the apical plasma membrane domain in epithelial cells.* J Cell Biol, 1988. **107**(5): p. 1717-28.
7. Yeaman, C., K.K. Grindstaff, and W.J. Nelson, *Mechanism of recruiting Sec6/8 (exocyst) complex to the apical junctional complex during polarization of epithelial cells.* J Cell Sci, 2004. **117**(Pt 4): p. 559-70.
8. Bagnat, M., et al., *Genetic control of single lumen formation in the zebrafish gut.* Nat Cell Biol, 2007. **9**(8): p. 954-60.

9. Kane, D.A., K.N. McFarland, and R.M. Warga, *Mutations in half baked/E-cadherin block cell behaviors that are necessary for teleost epiboly.* Development, 2005. **132**(5): p. 1105-16.

10. Ober, E.A., et al., *Mesodermal Wnt2b signalling positively regulates liver specification.* Nature, 2006. **442**(7103): p. 688-91.

11. Bryant, D.M. and J.L. Stow, *The ins and outs of E-cadherin trafficking.* Trends Cell Biol, 2004. **14**(8): p. 427-34.

12. D'Souza-Schorey, C., *Disassembling adherens junctions: breaking up is hard to do.* Trends Cell Biol, 2005. **15**(1): p. 19-26.

13. Le, T.L., A.S. Yap, and J.L. Stow, *Recycling of E-cadherin: a potential mechanism for regulating cadherin dynamics.* J Cell Biol, 1999. **146**(1): p. 219-32.

14. Palacios, F., et al., *Lysosomal targeting of E-cadherin: a unique mechanism for the down-regulation of cell-cell adhesion during epithelial to mesenchymal transitions.* Mol Cell Biol, 2005. **25**(1): p. 389-402.

15. Miyoshi, J. and Y. Takai, *Molecular perspective on tight-junction assembly and epithelial polarity.* Adv Drug Deliv Rev, 2005. **57**(6): p. 815-55.

16. Shimizu, T., et al., *E-cadherin is required for gastrulation cell movements in zebrafish.* Mech Dev, 2005. **122**(6): p. 747-63.

17. Omori, Y. and J. Malicki, *oko meduzy and related crumbs genes are determinants of apical cell features in the vertebrate embryo.* Curr Biol, 2006. **16**(10): p. 945-57.

18. Westerfield, M., *The Zebrafish Book: A guide for the Laboratory Use of Zebrafish (Danio rerio)*. 2000, Eugene, OR.

Figure Legends

Fig. A1.1 Lumen formation in polarity mutants

Transverse sections through the gut tube.

a, At 56hpf, *ava*^{tm94} ZMD larvae exhibit a multiple lumen phenotype(arrows).

b, At 72hpf, only a single lumen is observed in *ava*^{tm94} ZMD larvae.

c, Multiple lumens are also observed in the N-cadherin mutant *glo*^{m117}(arrows).

d, Single lumen is observed in the gut of crumbs2 mutant, *ome*^{m98} but the lumen is smaller.

Fig. A1.2 Epithelial polarization during gut morphogenesis in wildtype larvae

a, At 36hpf, cadherin is expressed in the cytoplasm and lateral membrane of gut epithelial cells. ZO-1 are localized in a few punctas that have clustered to the center of the radial pattern.

b, Cadherin expression becomes more restricted to the lateral membranes by 42hpf. However, there is still some cytoplasmic expression of cadherins. More ZO-1 positive punctas are present and they are present at most cell-cell contacts.

c, At 48hpf, cadherin is completely localized to the lateral membranes. Small lumens circumscribed by f-actin and ZO-1 punctas can be observed.

d, At 56hpf, cadherin is mostly localized to the subapical region with ZO-1 and actin foci. Single lumen is observed at this stage.

Fig. A1.3 Phenotypes of mutant FG7.3

a, Brightfield picture of wildtype and mutant larvae at 4dpf. Mutant larvae has a smaller head(arrow) and exhibit cardiac edema(arrowhead).

b-e, Transverse section through the anterior region of the gut tube of 5dpf larvae.

b, Expression of f-actin is decreased in the mutant larvae. In addition, the gut epithelium is thinner, the lumen is not expanded, and microvilli are not formed in the mutant larvae.

c, The apical marker 4B7 also marks the basal surface in the mutant gut.

d, Low levels of the basal marker 2H9 can be found on the apical surface and lateral domain of some cells in the mutant larvae.

e, 4E8 marks the apical domain in both wildtype and mutant larvae.

Fig. A1.4 Single lumen formation and expansion in the zebrafish gut tube.

Diagram depicting steps in single lumen formation and molecules involved in each step (boxed text). Green = cadherin. Red = ZO-1. Blue = f-actin.

a, At 36hpf, epithelial cells are in a disorganized state. Cadherin is expressed on cell-cell membranes in a broad expression pattern and in a punctated fashion around the perimeter of the gut. In addition, cadherin is found in the cytoplasm hypothesized to be endocytic trafficking vesicles (green dots). ZO-1 is expressed at some, but not all, vertices of cell-cell contact.

b, At 48hpf, cells are columnar in shape and have rearranged into a radial pattern. Expression of cadherin is more defined in the lateral membrane only. The basal surface is labeled by f-actin. Multiple small lumens have formed at the apical region of the

epithelial cells. These lumens are defined by f-actin and circumscribed by ZO-1 which is present at every cell-cell contact.

c, At 56hpf, the multiple lumens have coalesced to a single lumen. Cadherin expression becomes restricted to the subapical region of the lateral membrane. Minor expression is also found in the basal region. Apical membrane biogenesis occurs in order for lumen to expand.

Figure A1.1 Lumen formation in polarity mutants

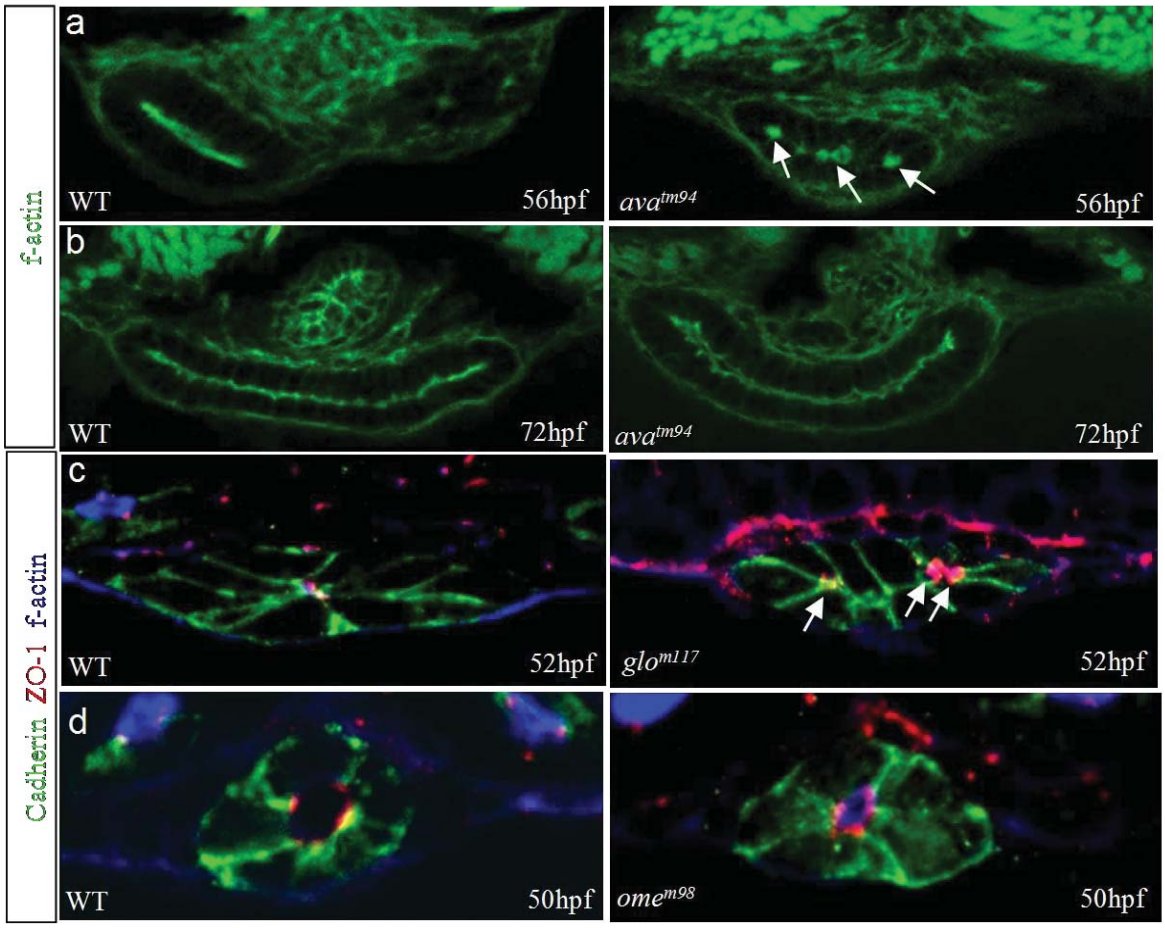

Figure A1.2 Epithelial polarization during gut morphogenesis in wildtype larvae

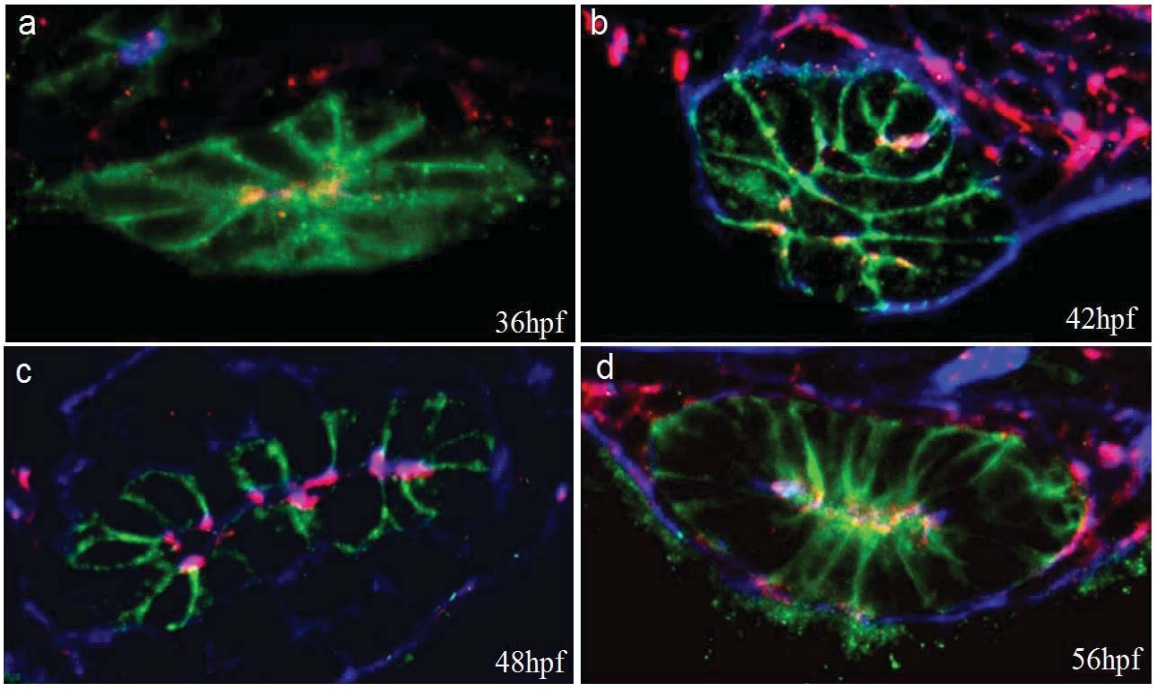

Figure A1.3 Phenotypes of mutant FG7.3

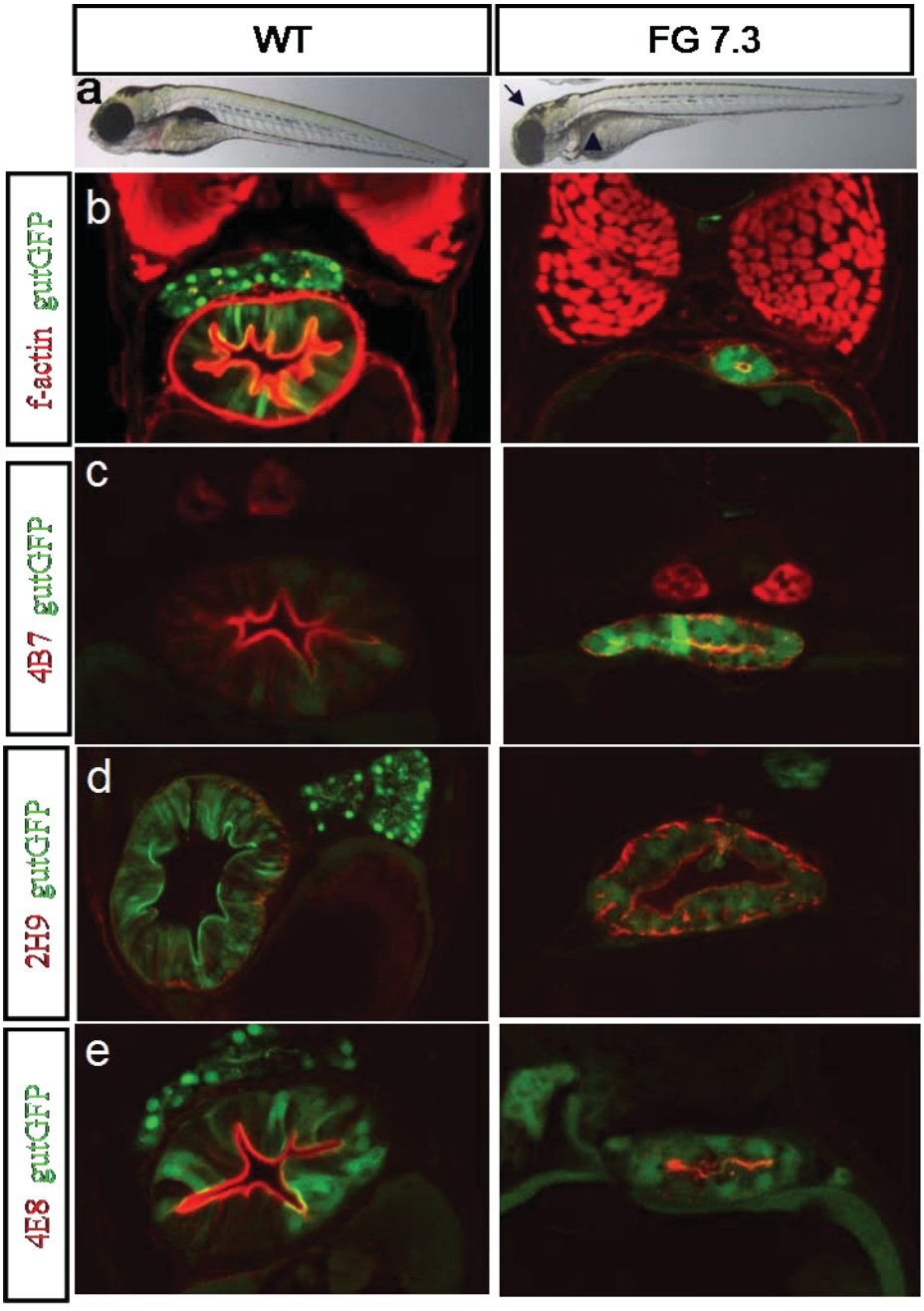

Figure A1.4 Single lumen formation and expansion in the zebrafish gut tube.

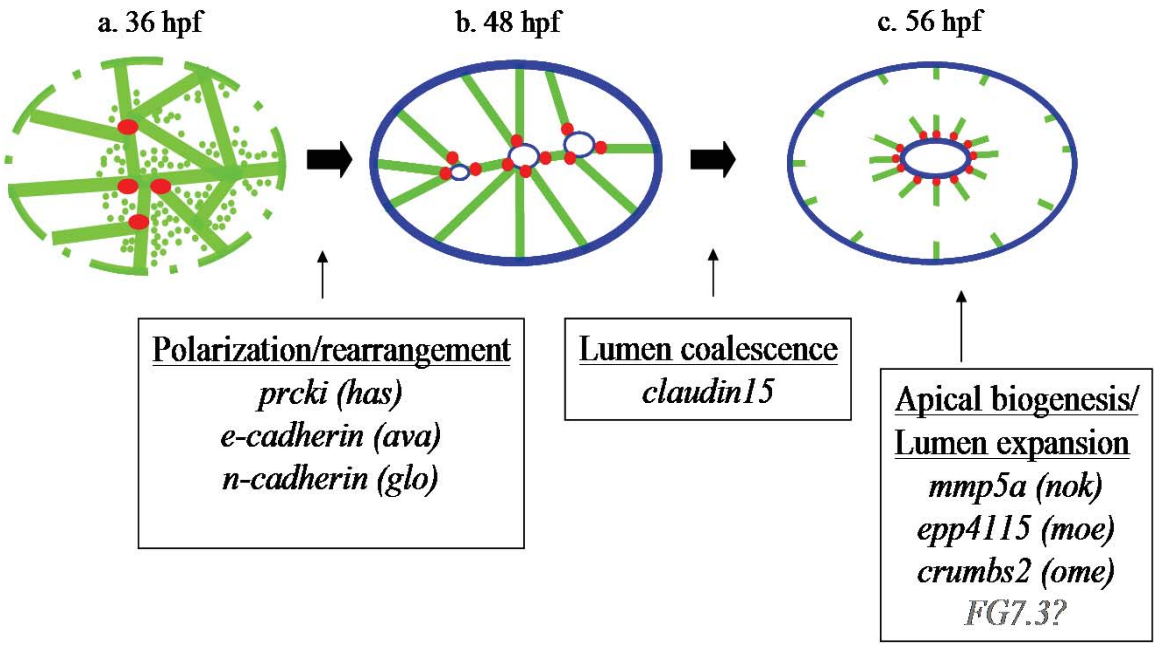

Appendix 2:

Novel Tg(lfabp:rasGFP) line as a tool to study liver development

Introduction

In mammalian liver development, many studies have focused on understanding transcription factors and signaling mechanism important for differentiation of hepatoblast to hepatocyte or biliary epithelial cells (BECs). While these understandings are important, identifying the cellular behaviors associated with differentiation can also help us understand the process better. For example, in mouse, formation of the bilayered ductal plate by hepatoblast is a crucial step in biliary differentiation.[1, 2]

While the zebrafish has proved to be a great model system to study liver development, there have been limitations in tools that can be used to study cellular behaviors during development. The antibodies against adhesion molecules cadherin and Alcam[3] have proved to be the most useful tool to visualize the cell shape of hepatoblasts, hepatocytes, and BECs. However, there are caveats associated with these tools.

During the early stages of liver development when all cells in the liver are hepatoblasts, the pan-cadherin antibody outlines the cell membrane of all hepatoblasts. At 2dpf, a subset of these cells has higher expression of cadherins. As development continues, cadherin expression in this subset of cells continues to intensify while it decreases in the other cells. This subset of cells is patterned similar to a tubular network. (personal communication, Silvia Curado) Thus, we hypothesized that cadherins are labeling hepatoblasts at early stages of development. Starting 48hpf when hepatoblast

are differentiating, hepatocytes slowly lose cadherin expression while BECs gain cadherin expression. At 4dpf, there are still low levels of cadherin in what is presumed to be hepatocytes. Besides the patterning phenotype, it has been difficult to distinguish between the two cells types. It is not until 5dpf that cadherin expression in hepatocytes is completely turned off. Similarly, Alcam is initially localized around the entire hepatoblast. Its expression becomes restricted to the apical membrane of hepatocytes at 60hpf.[3] Alcam is localized in the membrane of hepatocytes opposite of the side in contact with endothelial cells.[3] We believe that Alcam is outlining the biliary ductal network. Since Alcam is initially expressed in hepatoblast and becomes restricted to the apical region, it is unclear whether it is localized in hepatocytes or in BECs at 80hpf. Furthermore, if Alcam is indeed expressed in BECs, it would be interesting to know whether Alcam expression is turned off once the hepatoblast is differentiated to hepatocyte. It will be useful to have a marker that is only expressed in one of the two cell types at an earlier stage.

The liver fatty acid binding protein is an ideal marker for this purpose. RT-PCR detects expression of *lfabp* transcripts starting at 36hpf specifically in the liver.[4] Its expression continues to adulthood.[4] A 2.8kb 5'-flanking sequence of the zebrafish *lfabp* gene was isolated and shown to drive liver-specific expression starting at 2dpf.[4] Transgenic expression of fluorescent proteins driven by the 2.8kb *lfabp* promoter is in the hepatocytes only.[5] The lab currently has the Tg(lfabp:GFP) and Tg(lfabp:dsRed) lines but expression of these fluorescent proteins in the cytoplasm does not allow for analysis of cell membrane behaviors. Thus, I propose to generate a Tg(lfabp:rasGFP) line where GFP is tagged with the CAAX box of the Harvey Ras. The CAAX box is a signal

peptide that will target GFP to cell membranes. Generation of this transgenic line will be useful for furthering our understanding of liver development.

Results

I screened for germline-transmission of lfabp-rasGFP at 4dpf and identified two founders. Only one was deemed useful though as the other founder had extremely strong rasGFP signal in the liver which resulted in observation of rasGFP in the cytoplasm of hepatocytes (data not shown). This may be due to excessive insertions of the transgenic construct into the genome. Larvae from the 'useful' founder developed normally and had rasGFP expression in the liver only as observed under a dissecting microscope (Fig. A2.1a). Confocal analysis of the 4dpf larvae revealed that rasGFP only labels the cell membrane of hepatocytes. It did not label cells of other endodermal organs such as pancreas and gut (Fig. A2.1b). This is important because mouse *lfabp* is also expressed in the gut. However, confocal analysis revealed rasGFP expression on the membrane of skin cells (Fig. A2.1c). Expression in the skin was not as strong as that in the liver.

After identification of the transgenic founder, I continued to characterize the line. Expression of rasGFP was not detected at 26hpf. (data not shown) At 32hpf, I observed rasGFP signal that co-localizes with liver marker Prox1. (Fig. A2.2a) Each cell in the developing liver bud was outlined by rasGFP. Three-dimensional reconstruction of the endoderm at 42hpf and 50hpf revealed that rasGFP is only expressed in the liver (Fig. A2.2b-c). Single plane confocal images of the same stage showed that the liver expression of rasGFP is localized to the entire membrane of cells in the liver (Fig. A2.2d-f). Minor expression of rasGFP was detected in some regions of the gut (Fig. A2.2e, data not shown). Furthermore, analysis with pan-cadherin and ZO-1 antibodies highlighted the developing ductal structure. (Fig. A2.2d-f, middle column). Interestingly, the region

where the extrahepatic duct entered the liver and transitioned to the intrahepatic duct was devoid of rasGFP (Fig. A2.2d, arrow).

To further understand cadherin and Alcam expression in the developing liver, I co-stained these two markers in the Tg(lfabp:rasGFP) line. At 60hpf, both cadherin and Alcam colocalized with rasGFP. They labeled all cell types in the liver and they outlined the entire cell membrane (Fig. A2.2g'). However, at 72hpf, localization of these proteins changed. Alcam expression became restricted to a special population of cells that also exhibited enhanced pan-cadherin signal (Fig. A2.2h'). This population of cells is located near the surface of hepatocytes where there is a lower expression of rasGFP (Fig. A2.2h'). It is important to note that there is no co-localization of Alcam and rasGFP as was observed at 60hpf (Fig. A2.2g', h'). Alcam-positive cells are arranged into a more tubular pattern at 80hpf (Fig. A2.2i'). RasGFP continues to be expressed differentially on the cell membrane of all hepatocytes (Fig. A2.2i'). By 4dpf, expression of Alcam and cadherin have completely segregated from rasGFP (Fig. A2.2j'). Differential expression of rasGFP is more pronounced at this stage. Expression of rasGFP on the apical side near Alcam and cadherin expression (Fig. A2.2j', arrowhead) is much lower as compared to expression on the basal side (Fig. A2.2j', arrows). A projection of Tg(lfabp:rasGFP) showed that the enhanced rasGFP expression lines 'holes' and 'tracks' in the liver (Fig. A2.2j'', asterisks). Expression of Tg(lfabp:rasGFP) and Tg(flk1:mCherry), which marks the vasculature, together show that the holes and tracks outlined by rasGFP is occupied by the vasculature (data not shown).

Discussion and Future Directions

Here, I report the successful generation of a transgenic line that proves to be a useful tool for studying liver development. The promoter region of *lfabp* gene was used to drive the expression of the membrane-bound GFP (rasGFP). The expression profile of this transgene recapitulates what have been described.[4] Expression of rasGFP in the liver can be detected under a dissection microscope with fluorescence at 2dpf. However, confocal microscopy reveals that rasGFP expression on the entire cell membrane begins as early as 32hpf. This expression continues through 60hpf. Starting at 72hpf, rasGFP is no longer expressed in ductal cells. Instead, it is only expressed in hepatocytes in a differential expression pattern where the rasGFP signal is more intense on the basal surface as compared with the apical surface. It is important to note that Alcam and pan-cadherin which lines the apical region of hepatocytes do not co-localize with rasGFP at later stages of development when BECs are fully differentiated. Also, the region of the liver where the intrahepatic duct connects with the extrahepatic duct is devoid of rasGFP, even at early stages such as 42hpf. These data suggest that rasGFP driven by the *lfabp* promoter is not expressed in ductal cells.

The new transgenic line helped identify the type of cells the Alcam and pan-cadherin antibodies were labeling. Since Alcam initially co-localizes with Tg(lfabp:rasGFP) but subsequently segregates from it, it is likely that Alcam is expressed in hepatoblast in the early stages of development. Then, its expression is turned off in the hepatocytes and remains on in BECs after differentiation. Since the change in expression profile is so distinct, it is possible that Alcam may play a role in the differentiation of hepatoblast to BECs. Conversely, the change in cadherin expression profile is gradual.

This might be due to the fact that a pan-cadherin antibody was used. This antibody may be detecting a multitude of cadherins that are expressed in liver cells so the expression pattern observed is broader. From the high resolution magnified image of 4dpf larvae (Fig. A2.2j', arrowhead), it is clear that there is a space between the membrane of BECs and hepatocytes. From these experiments, it can be concluded that the pan-cadherin antibody, along with Alcam, labels the cell membrane of BECs and not the apical membrane of hepatocytes as previously thought. An interesting question would be to address whether the changes in protein expression pattern has any significance in differentiation and patterning.

With additional characterization of Alcam and pan-Cadherin in the novel Tg(Tp1bglob:eGFP) line, we can compare it to data reported here to obtain a better understanding of how cells behave during differentiation and patterning of the liver. In addition, we are currently generating a Tg(Tp1bglob:ras-mCherry) line to label the cell membrane of all BECs red. Having the lfabp:rasGFP and tp1bglob:ras-mCherry transgenes together will beautifully highlight the cell membrane of each cell type. It may provide insights into cellular behaviors during the differentiation of hepatoblasts to hepatocytes or BECs.

An unexpected result from the Tg(lfabp:rasGFP) is that it also marks the location of the vasculature. Both hepatocytes and vasculature can be marked by one color. This will be beneficial for subsequent studies since it will free up more fluorophore colors to study additional protein or structure. It is important to note that the labeling of hepatocyte cell membrane may be very confusing at stages after 4dpf because there are

too many hepatocytes in the liver. It may be hard to draw definite conclusions from experiments with this transgenic line after 4dpf unless the imaging protocol is optimized.

Materials and Methods

Animals. AB wild-type and transgenic fish were maintained as described previously.[6]

Generation of transgenic construct. The rasGFP was cloned into I-Sce vector (BiSKi) with NcoI/NotI. Then, the 2.8kb lfabp promoter fragment was cloned into I-Sce vector with EcoRI/SalI.

Generation of stable transgenic zebrafish. The I-Sce meganuclease recombination system was used to generate the Tg(lfabp:rasGFP). The lfabp-rasGFP construct was injected into one-cell stage wildtype embryos to produce germline-transmitting transgenic zebrafish lines. The injected embryos were grown to adulthood. The adult fish were then crossed to wildtype to identify germline-transmitting transgenic founders.

Immunohistochemistry. Larvae were fixed in 4% formaldehyde in egg water at 4°C overnight. The fixed larvae were washed in PBS and embedded in 4% low-melt agarose in PBS. Transverse sections 200μm thick were obtained with a vibratome (Leica, Bannockburn, IL, USA). Sections were incubated with primary antibodies overnight at 4°C. Sections were then washed and incubated with Alexa Fluor conjugated secondary antibodies or Alexa Fluor conjugated phalloidin. After washing, sections were mounted on slides in Vectashield and imaged on a Zeiss LSM510 Pascal confocal microscope. Images were further analyzed with LSM software (Zeiss, Thornwood, NY, USA) and Image J Software.

References

1. Antoniou, A., et al., *Intrahepatic bile ducts develop according to a new mode of tubulogenesis regulated by the transcription factor SOX9.* Gastroenterology, 2009. 136(7): p. 2325-33.
2. Zong, Y., et al., *Notch signaling controls liver development by regulating biliary differentiation.* Development, 2009. 136(10): p. 1727-39.
3. Sakaguchi, T.F., et al., *Endothelial signals modulate hepatocyte apicobasal polarization in zebrafish.* Curr Biol, 2008. 18(20): p. 1565-71.
4. Her, G.M., et al., *In vivo studies of liver-type fatty acid binding protein (L-FABP) gene expression in liver of transgenic zebrafish (Danio rerio).* FEBS Lett, 2003. 538(1-3): p. 125-33.
5. Curado, S., et al., *The mitochondrial import gene tomm22 is specifically required for hepatocyte survival and provides a liver regeneration model.* Dis Model Mech. 3(7-8): p. 486-95.
6. Westerfield, M., *The Zebrafish Book: A guide for the Laboratory Use of Zebrafish (Danio rerio)*. 2000, Eugene, OR.

Figure Legends

Fig. A2.1 Identification of a Tg(lfabp:rasGFP) founder

a, Brightfield picture of a 4dpf larvae with expression of rasGFP in the liver. Development of the larvae appears normal.

b, Confocal analysis of a whole-mount larvae at 4dpf. Ventral view of endoderm. rasGFP is only expressed in the liver(L). Pancreas(P) and gut(G) do not express rasGFP.

c, Confocal analysis of the head region of the same larvae as (b). There is a low level of rasGFP expression in the skin.

Fig. A2.2 Characterization of Tg(lfabp:rasGFP)

a, Expression of rasGFP is observed at 32hpf. It co-localizes with liver marker Prox1.

b-c, Projections of confocal images of 42hpf and 50hpf transgenic larvae. rasGFP is expressed in the liver bud. Pan-cadherin antibody outlines the endoderm. Liver(L), Pancreas(P), Gut(G)

d, Single confocal plane of 42hpf transgenic larvae. Expression of rasGFP in the liver bud. Pan-cadherin antibody outlines the endoderm and highlights the initial intrahepatic ductal structure that connects from the extrahepatic duct(arrow). rasGFP is absent from this location. ZO-1 co-localizes with this ductal structure.

e, Single confocal plane of 50hpf transgenic larvae. Expression of rasGFP continues in the liver bud and co-localizes with pan-Cadherin. ZO-1 is localized to regions of enhanced pan-Cadherin, usually in the center of the liver.

f, Single confocal plane of 55hpf transgenic larvae. rasGFP continues to be localized with pan-cadherin and expression of ZO-1 is more scattered throughout the liver.

g-i, Projections of confocal images of the liver at 60hpf, 72hpf, and 80hpf. rasGFP is expressed in the entire liver. The biliary ductal network is outlined by Alcam.

g'-i', Single confocal plane. Magnified view of the boxed regions in (g-i).

g', At 60hpf, all three markers (rasGFP, Alcam, and pan-cadherin) labels the entire cell membrane of all cells in the liver. rasGFP is not expressed in the region where extrahepatic duct enters the liver.

h', At 72hpf, Alcam labels only a subset of cells. Cadherin labels all cell in the liver but its expression in the subset of cells is enhanced. rasGFP continues to label all liver cells but cells have decreased expression of rasGFP on one of its surfaces (arrow). This surface coincides with Alcam and where cadherin expression is increased. There is no co-localization of all three markers anywhere in the liver.

i', At 80hpf, Alcam labels cells that are arranged in a tubule network pattern. Pan-cadherin continues to label all cells in the liver but expression is enhanced in Alcam positive cells. rasGFP continues to be expressed in all Alcam negative cells in a differential pattern(arrow).

j, Single confocal plane of the liver at 4dpf. rasGFP labels all hepatocytes in the liver. Alcam and pan-cadherin label the biliary ducts. The regions not labeled by rasGFP(*) are where the vasculature is located. Gut (G)

j', Single confocal plane of the boxed region in (j). Differential expression of rasGFP in hepatocytes. There is less signal on the side neighboring the biliary ducts(arrowhead) and enhanced signal on the opposite side outlining the holes(arrows). Alcam and pan-cadherin marking BECs do not co-localize with rasGFP.

j'', Projection of confocal images of the hashed-boxed region in (j). Pan-cadherin and Alcam labels the biliary ductal network. The vasculature can be visualized by the 'holes' and 'tracks' outlined by the enhanced rasGFP signal. 'Holes' are marked by *.

Figure A2.1 Identification of a Tg(lfabp:rasGFP) founder

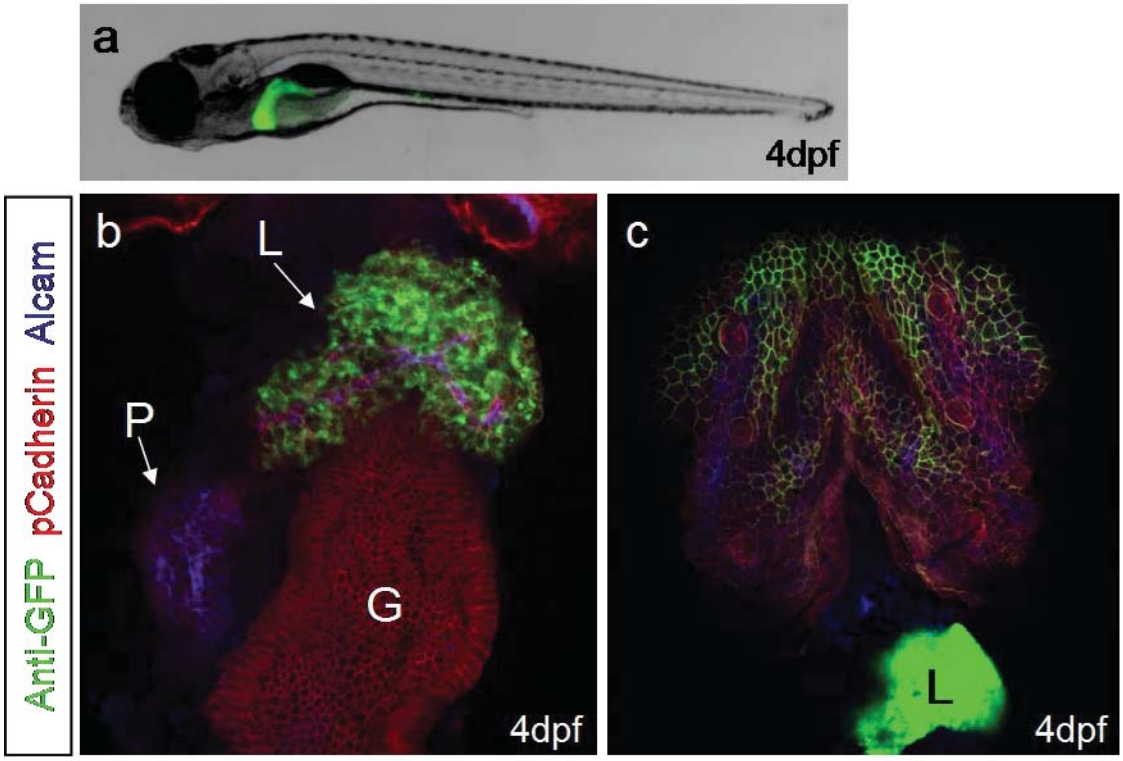

Figure A2.2 Characterization of Tg(lfabp:rasGFP)

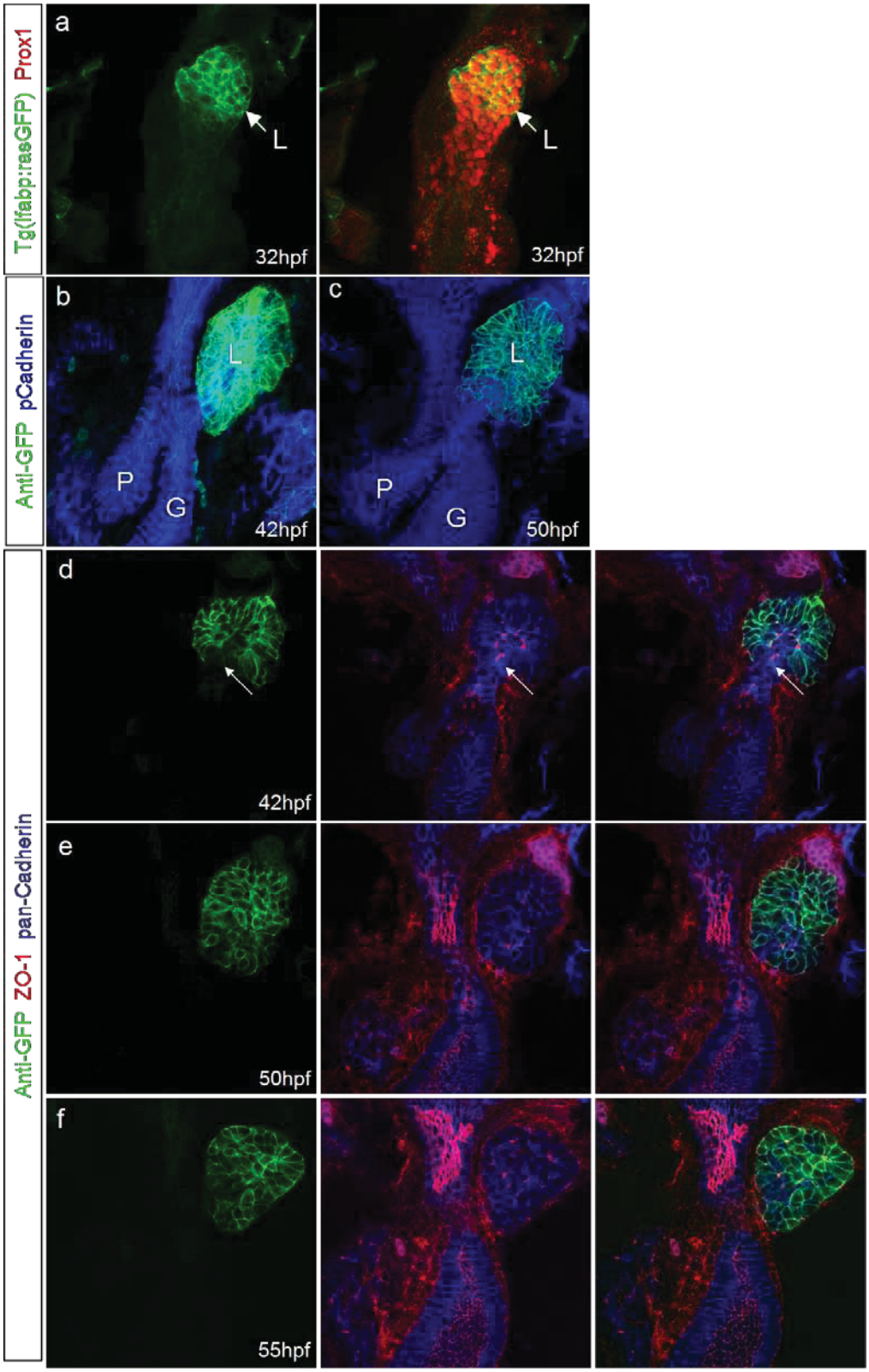

Figure A2.2 Characterization of Tg(lfabp:rasGFP) – continued

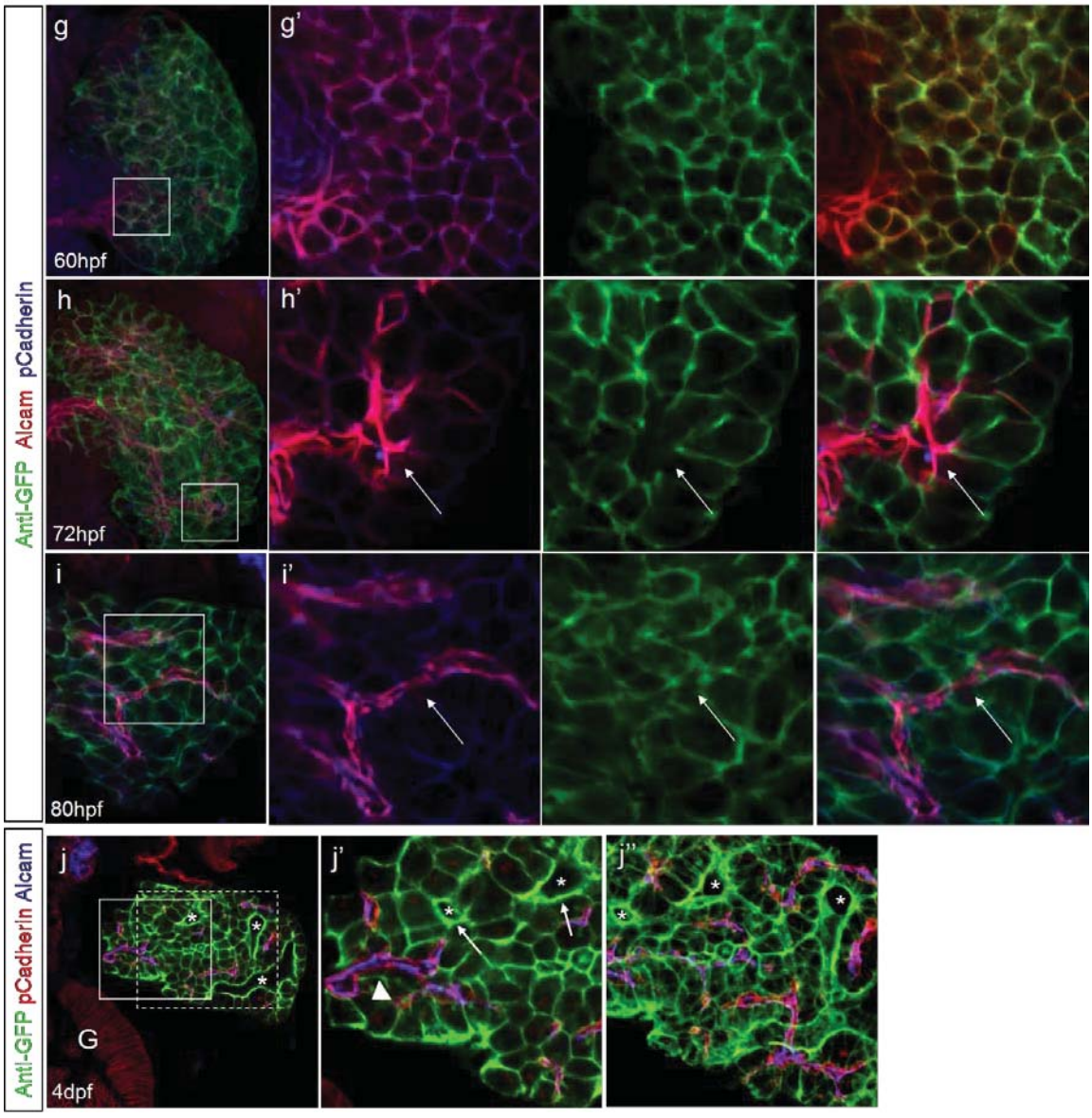

UCSF Library Release

Publishing Agreement
It is the policy of the University to encourage the distribution of all theses, dissertations, and manuscripts. Copies of all UCSF theses, dissertations, and manuscripts will be routed to the library via the Graduate Division. The library will make all theses dissertations, and manuscripts accessible to the public and will preserve these to the best of their abilities, in perpetuity.

Please sign the following statement:
I hereby grant permission to the Graduate Division of the University of California, San Francisco to release copies of my thesis, dissertation, or manuscript to the Campus Library to provide access and preservation, in whole or in part, in perpetuity.